Clinical Science (2025) **139** 1261–1285
https://doi.org/10.1042/CS20257272

Research Article

Low- and high-dose post-transplant cyclophosphamide attenuates graft-versus-host disease with distinct effects on PD-1$^+$ T cell subsets

Chloe Sligar, Miles J. Jacobs, Amal Elhage, Ronald Sluyter and Debbie Watson

[1]Molecular Horizons and School of Science, University of Wollongong, Wollongong, NSW, 2522, Australia

Correspondence: Debbie Watson (dwatson@uow.edu.au)

OPEN ACCESS

Allogeneic haematopoietic stem cell transplantation (alloHSCT) is a curative treatment for haematological malignancies. AlloHSCT aims to generate graft-versus-leukaemia immunity, where donor T cells eliminate residual malignant cells. However, graft-versus-host disease (GVHD), where donor T cells attack recipient tissues, is a common and often fatal side effect. Post-transplant cyclophosphamide (PTCy) can reduce GVHD, but the cellular mechanisms through which this occurs are not fully understood, and high doses may be associated with toxicity. This study aimed to determine whether lower doses of PTCy can reduce GVHD and to examine the effects of PTCy doses on human (h) immune cell subsets, T cell exhaustion, and histological GVHD in a humanised mouse model. NOD-*scid*-IL2Rγ^{null} mice were injected with 2×10^7 human peripheral blood mononuclear cells on day 0, cyclophosphamide (10, 25 or 33 mg/kg) or control diluent on days 3 and 4 and monitored for GVHD development at early and late time points. Low-dose PTCy (10 mg/kg) abrogated clinical signs of GVHD with comparable efficacy to high-dose PTCy (33 mg/kg), delaying GVHD onset and prolonging mouse survival. Proportions of hPD-1$^+$ hCD4$^+$ and hPD-1$^+$hCD8$^+$ T cells were increased with low-dose PTCy but not higher doses, while hPD-1$^+$ hTreg proportions were increased by all PTCy doses. Exhausted hPD-1$^+$hLAG3$^+$hCD8$^+$ T cell proportions were increased with high-dose PTCy, but not lower doses. This study indicates that low-dose PTCy reduces GVHD with similar efficacy to that of high-dose PTCy, but this appears to be associated with differing cellular mechanisms of action.

Introduction

Allogeneic haematopoietic stem cell transplantation (alloHSCT) is a curative treatment for haematological malignancies, including leukaemia, that are refractory to chemotherapy and radiotherapy [1]. Following myeloablation, alloHSCT aims to generate graft-versus-leukaemia (GVL) immunity, where alloreactive donor T cells in the graft eliminate residual host malignant cells [2]. Despite its effectiveness, this treatment is frequently associated with graft-versus-host disease (GVHD), where alloreactive donor T cells also recognise the healthy tissues of the transplant recipient as foreign and mount a destructive inflammatory immune response [3]. GVHD results in severe damage to multiple organs, including the skin, liver, gastrointestinal tract and lungs [3–5]. One therapeutic strategy for the prevention of GVHD is the use of post-transplant cyclophosphamide (PTCy). While PTCy reduces GVHD occurrence and severity, this disease still develops in 40–50% of patients [6,7], and the cellular mechanisms of action by which PTCy reduces the disease are not fully understood.

In alloHSCT, PTCy is commonly delivered on days 3 and 4 post-transplant at a high dose (≥50 mg/kg), where it reduces GVHD [8–10]. Although inexpensive and effective in most cases, the administration of PTCy has been associated with impaired immune reconstitution [11–13] and toxicity [14]. Common toxicities associated with high doses of cyclophosphamide include cardiotoxicity [15], liver toxicity [16], gonadal and ovarian failure and haemorrhagic cystitis and fibrosis in the bladder [14]. Furthermore, cyclophosphamide is carcinogenic and can lead to bladder cancer, secondary acute leukaemia and kidney cancer [17,18], with higher cyclophosphamide doses associated with a greater incidence of these adverse events and increased patient mortality [16]. As such, the efficacy of low-dose PTCy following alloHSCT is now being explored.

Received: 2 June 2025
Revised: 30 September 2025
Accepted: 6 October 2025

Version of Record Published: 28 October 2025

© 2025 The Author(s). This is an open access article published by Portland Press Limited on behalf of the Biochemical Society and distributed under the Creative Commons Attribution License 4.0 (CC BY).

Clinical Science (2025) **139** 1261–1285
https://doi.org/10.1042/CS20257272

In allogeneic mouse models, one study by Wachsmuth and colleagues found lower doses of PTCy (10 mg/kg and 25 mg/kg) reduced GVHD, with the latter being superior in reducing GVHD mortality, decreasing alloreactive $CD4^+$ and $CD8^+$ T cells and increasing donor regulatory T cells (Tregs) compared with both lower (10 mg/kg) and higher (50–200 mg/kg) PTCy doses [19]. Another study by Wang and colleagues found that low-dose PTCy (10 mg/kg) was able to mitigate GVHD, indicating a role for donor Treg reconstitution in this outcome [20].

Clinically, a low dose of PTCy (14.5 mg/kg) on days 3 and 4 post-transplant in combination with anti-thymocyte globulin significantly reduced the cumulative incidence of severe acute GVHD compared with anti-thymocyte globulin alone; however, 30% of these patients still developed moderate to severe chronic GVHD [21]. More recently, another clinical study involving elderly patients undergoing haploidentical alloHSCT revealed that PTCy at a lower dose (40 mg/kg) was found to have a similar efficacy to that of a high dose (50 mg/kg); however, 32% of patients administered this lower dose still developed GVHD, with 52% achieving GVHD-free, relapse-free survival at two years post-transplant [22].

Despite being used clinically for over a decade, the precise mechanism by which PTCy at high or low doses reduces GVHD and impacts alloreactive donor T cells remains unclear. Some proposed mechanisms of action include the depletion of proliferating effector T cells [23], the induction of effector T cell dysfunction or exhaustion [19], or the enhancement of Treg survival and function [24]. T cell exhaustion refers to a dysfunctional state induced by chronic antigen exposure, characterised by the gradual decline of T cell effector functions and self-renewal capacity [25,26]. PD-1 (or programmed cell death protein 1) is an inhibitory receptor present on activated T cells and plays a key role in modulating immune responses [27,28]. LAG3 (or lymphocyte activation gene 3) is expressed on multiple T cell subsets and is involved in T cell homeostasis, activation and proliferation [29]. T cells that co-express both PD-1 and LAG3 are considered exhausted, resulting in loss of effector functions and cell death due to overstimulation [30]. While exhausted effector T cells may be beneficial in the context of GVHD, the opposite may be true for generating GVL immunity. In an allogeneic mouse model of GVL immunity, T cell exhaustion was found to contribute to reduced GVL responses, which could be overcome via PD-1 blockade, but not via blockade of other exhaustion-associated receptors, including LAG3 [31]. Moreover, an association between $CD4^+$ and $CD8^+$ T cell exhaustion and relapse has been identified in patients with acute myeloid leukaemia [32] and B-cell acute lymphoblastic leukaemia [33]. As such, the impact of PTCy on T cell exhaustion warrants further investigation.

An imbalance of effector T cells and Tregs is associated with the development of GVHD following alloHSCT [34]. Tregs protect against GVHD through the secretion of regulatory cytokines, including interleukin (IL)-10, IL-35 and transforming growth factor beta [35,36], and through the overexpression of immune checkpoint inhibitors such as PD-1 [37]. In allogeneic mouse models, PD-1-deficient Tregs showed increased apoptosis, reducing Treg numbers and worsening GVHD [38]. This study also showed that a single 50 mg/kg dose of PTCy on day 3 post-transplant rescued PD-1 deficient Tregs from apoptosis, re-establishing the balance between regulatory and effector T cells through depletion of alloreactive T cells while sparing Tregs that are resistant to PTCy effects due to the expression of aldehyde dehydrogenase [6].

This study aimed to determine whether lower doses of PTCy (10 mg/kg and 25 mg/kg) are equally as efficacious as high-dose PTCy (33 mg/kg) in limiting GVHD in a preclinical humanised mouse model. This study also aimed to explore the cellular mechanisms of action by which different PTCy doses reduce GVHD by examining the impact of PTCy at each dose on human (h) immune cell subsets, with a focus on markers of T cell exhaustion at early and late disease time points in this preclinical model.

Methods

Mice

Approval for experiments involving mice was obtained from the University of Wollongong (Wollongong, Australia) Animal Ethics Committee (AE 20/01). Female, 5–7-week-old NOD-*scid*-IL2Rγ^{null} (NSG) (n=60 total; n=10 per treatment group for the long-term model and n=5 per treatment group for the short-term model) mice were obtained from Australian BioResources (Moss Vale, Australia) and housed in the Molecular Horizons Animal Research Facility, University of Wollongong. Mice, each from different treatment groups, were housed in individually ventilated cages (Tecniplast, Buggiate, Italy) under a 12 h light/12 h dark cycle, with four mice per cage. In alignment with the 3Rs, female mice were used to allow for group co-housing, as male mice are prone to aggression when co-housed [39]. Mice were provided with

© 2025 The Author(s). This is an open access article published by Portland Press Limited on behalf of the Biochemical Society and distributed under the Creative Commons Attribution License 4.0 (CC BY).

enrichments, irradiated mouse chow (Specialty Feeds, Glen Forrest, Australia) and autoclaved water *ad libitum*. Mice were acclimatised for two weeks before commencing experiments.

Human peripheral blood mononuclear cell isolation

Approval for experiments involving human blood was obtained from the University of Wollongong Human Ethics Committee (HE 12/290) and with consent from healthy human donors (two females and four males, aged 21–30 years). Human peripheral blood mononuclear cells (hPBMCs) were isolated by density gradient centrifugation (562×***g***, 30 min; break disengaged) using Ficoll-Paque PLUS (GE Healthcare, Uppsala, Sweden). hPBMCs were washed twice with sterile Dulbecco's phosphate buffered saline (PBS) (Thermo Fisher Scientific, Waltham, U.S.A.) (440×***g***, 10 min) and resuspended in PBS at 1×10^8 cells/ml for injection into mice.

Humanised mouse model of GVHD

NSG mice were then injected intraperitoneally (i.p.) with 2×10^7 hPBMCs (day 0) from different donors (n=2–6 donors per experiment, described in detail in corresponding figure legends) using a 27-gauge × 12 mm needle and 1 ml syringe. Cyclophosphamide (40 mg/ml; Sigma Aldrich, St Louis, U.S.A.) was diluted to 6.6, 5 or 2 mg/ml with PBS and stored for up to 48 h at 4°C prior to injection. On days 3 and 4, mice were injected i.p. with either cyclophosphamide (33 mg/kg, 25 mg/kg or 10 mg/kg) or PBS using a 30-gauge × 8 mm insulin syringe. Mice were monitored and scored in a blinded fashion at least thrice weekly until endpoint as described [40], with mice euthanised by slow-fill CO_2 at day 28 (short-term model), day 70 (long-term model) or ethical endpoint. Organs (spleen, liver, lung, ear and skin) were collected into PBS, RPMI-1640 medium (Thermo Fisher Scientific) and/or 10% neutral buffered formalin (Sigma Aldrich) as indicated.

Histology

Livers, lungs, skin and ears collected from euthanised mice were fixed overnight in 10% neutral buffered formalin. Tissues were processed in an ASP200S tissue processor (Leica, Buffalo Grove, U.S.A.) and embedded in paraffin wax before being sectioned (3–5 µm) using an RM2255 microtome (Leica) and stained with haematoxylin and eosin (POCD, Artarmon, Australia) (Table 1). Histopathology was assessed using a DM750 inverted light microscope (Leica) with the 20X objective and Leica Application Suite software version 4.7 (Leica). Liver, skin and ear histopathology were assessed in a blinded manner using a standardised grading system (grades 0–4) as described [41]. Lung histopathology was assessed in a blinded manner by area measurements of open alveolar space using Fiji [42] and quantified as a percentage of the total measured lung area.

Immunophenotyping

Cells were isolated from spleens and livers as described [43] before live/dead staining with Zombie near infrared (NIR) dye (BioLegend, San Diego, U.S.A.). Cells were then incubated with fluorochrome-conjugated monoclonal antibodies (Table 2) in PBS containing 2% foetal calf serum for 10 min on ice, protected from light. Cells were washed in PBS (300×***g***, 5 min) and resuspended in 250 µl PBS for flow cytometric data acquisition. Data were obtained using an LSRFortessa X-20 flow cytometer (BD Biosciences, San Jose, U.S.A.) using the appropriate lasers and band-pass filters (Table 2) and FACSDiva software version 8 (BD Biosciences). Data were analysed using FlowJo software version 10 (BD Biosciences) with gating based on fluorescence minus one controls and populations defined as shown (Table 3).

Data presentation and statistical analysis

Data are presented as the mean ± standard error of the mean. Data from mice that were euthanised prior to experimental endpoint were carried forward. Mice (n=7) with <5% human $CD45^+$ cells in tissues examined by flow cytometry were considered non-engrafted and excluded from analyses. Data sets were tested for normality with a Shapiro–Wilk test. Statistical differences for multiple comparisons were analysed using one-way analysis of variance (ANOVA) with Dunnett's post-hoc (parametric) or Kruskal–Wallis with Dunn's multiple comparisons correction (non-parametric) tests. Statistical differences in clinical score and weight over time were assessed using a repeated measures two-way ANOVA with Geisser–Greenhouse

© 2025 The Author(s). This is an open access article published by Portland Press Limited on behalf of the Biochemical Society and distributed under the Creative Commons Attribution License 4.0 (CC BY).

Clinical Science (2025) **139** 1261–1285
https://doi.org/10.1042/CS20257272

Table 1: Haematoxylin and eosin staining protocol

Step	Reagent	Time (sec)
1	Xylene substitute	150
2	100% ethanol	100
3	Water	120
4	Haematoxylin	100
5	Water	120
6	Acid alcohol (1% HCl in 100% ethanol)	1[1]
7	Water	60
8	Scott's bluing reagent (45 mM $NaHCO_3$, 166 mM $MgSO_4$)	60
9	Water	60
10	Eosin	20
11	100% ethanol	105
12	Xylene substitute	70

[1]Slides were dipped once in acid alcohol.

Table 2: Reagents used for immunophenotyping

Target	Clone	Fluorochrome	Excitation wavelength (nm)	Band pass filter wavelength (nm)
hCD127	HIL-7R-M21	BV421	405	450/50
hCD3	UCHT1	BV510	405	525/50
hCD161	HP-3G10	BV605	405	610/20
hCD279 (PD-1)	EH12.1	BV605	405	610/20
hCD183	1C6/CXCR3	BV711	405	710/50
hCD45	HI30	FITC	488	525/15
hCD158e1 (KIR)	DX9	FITC	488	525/15
mCD45	30-F11	PerCP	488	695/40
hCD4	SK3	PerCP-Cy 5.5	488	695/40
hCD25	M-A251	PE	561	586/15
hCD8	RPA-T8	PE-Cy7	561	780/60
hCD56	B159	PE-Cy7	561	780/60
hCD39	TU66	APC	640	670/30
hCD223 (LAG3)	7H2C65	APC	640	670/30
Live/dead stain		Zombie NIR dye	640	780/60

All fluorochrome-conjugated monoclonal antibodies were obtained from BD Biosciences except for CD158e1 and CD223, which were from BioLegend.
APC, allophycocyanin. BV, Brilliant Violet. FITC, fluorescein isothiocyanate. PE, R-phycoerythrin. PE-Cy7, phycoerythrin-cyanine 7. PerCP, perdinin chlorophyll protein-cyanine. PerCP-Cy 5.5, peridinin chlorophyll protein-cyanine5.5. h, human. m, mouse. NIR, near infrared..

correction. Statistical differences in survival were assessed using a Mantel–Cox test. P values ≤ 0.1 are reported on graphs. P values reported in the corner of weight, clinical score and survival graphs represent the difference between all treatment groups. Statistical analyses and graphs were produced using GraphPad Prism software version 9 (GraphPad Software, La Jolla, U.S.A.). Differences were considered significant where $P<0.05$.

Results

Low-dose PTCy prolongs time to GVHD onset in humanised NSG mice

Our group has previously shown that high-dose PTCy (33 mg/kg) on days 3 and 4 reduces but does not prevent GVHD in humanised NSG mice, acting through the depletion of proliferating T cells observed at day 6 [44]. However, high-dose PTCy is associated with toxicity risks [15,16,45]. To determine whether

© 2025 The Author(s). This is an open access article published by Portland Press Limited on behalf of the Biochemical Society and distributed under the Creative Commons Attribution License 4.0 (CC BY).

Table 3: Markers used to define immune cell populations

Population	Markers used to define population
$hCD45^+$	$hCD45^+mCD45^-$
$hCD3^+$	$hCD45^+hCD3^+$
$hCD4^+$	$hCD45^+hCD3^+hCD4^+$
$hCD8^+$	$hCD45^+hCD3^+hCD8^+$
hTregs	$hCD45^+hCD3^+hCD4^+hCD127^{low}hCD25^+$
$hCD39^+$hTregs	$hCD45^+hCD3^+hCD127^{low}hCD25^+hCD39^+$
hTcons	$hCD45^+hCD3^+hCD4^+$ cells excluding hTregs
hTh17	$hCXCR3^-hCD161^+$ hTcons
hTh1	$hCXCR3^+hCD161^-$ hTcons
hTc17	$hCD45^+hCD3^+hCD8^+hCD161^{high}$
$hKIR^+hCD8^+$	$hCD45^+hCD3^+hCD8^+hCD158e1^+$
hUnconv T	$hCD45^+hCD3^+hCD56^+$
hNK	$hCD45^+hCD3^-hCD56^+$

h, human. Treg, regulatory T cell. Th, T helper. Tc, cytotoxic T. Uncov, unconventional. NK, natural killer. Tcon, conventional T. KIR, killer cell immunoglobulin-like receptor.

lower doses of PTCy could attenuate GVHD, NSG mice were injected i.p. with 2×10^7 hPBMCs (from six healthy donors) on day 0. Mice then received i.p. injections of PTCy at a low dose (10 mg/kg; PTCy 10), mid dose (25 mg/kg; PTCy 25) or high dose (33 mg/kg; PTCy 33) or PBS for control (Ctrl) mice on days 3 and 4. A dose of 33 mg/kg PTCy was considered high-dose due to the established use of this dose in this model, mechanistic relevance and tolerability rather than direct mg/kg equivalence to the clinical 50 mg/kg dose. Mice were subsequently monitored for up to 70 days for clinical signs of GVHD (Figure 1A).

Weight loss was observed in Ctrl mice from day 12, whereas PTCy 33 mice gained weight until day 30 before steadily declining in weight until endpoint (Figure 1B). PTCy 10 mice gained weight until day 20 before plateauing and maintaining weight until endpoint, whereas PTCy 25 mice began to lose weight from day 12, similar to Ctrl mice. However, the overall difference between groups was not statistically significant (P=0.15).

Clinical scores of Ctrl, PTCy 10 and PTCy 25 mice increased from day 9, whereas there was a delayed increase in the clinical scores of PTCy 33 mice, beginning at day 30. Nevertheless, the overall difference between groups was not statistically significant (P=0.46) and all mice had similar clinical scores at endpoint (P=0.35) (Figure 1C).

Time to GVHD onset (defined as a clinical score ≥ 3) [46] was similar between Ctrl (23 days) and PTCy 25 mice (28 days) (P=0.55). When compared with Ctrl mice, time to GVHD onset was significantly delayed in PTCy 10 (36 days) (P=0.03) and PTCy 33 mice (37 days) (P=0.04) (Figure 1D).

Ctrl mice had a median survival time (MST) of 27 days. Comparatively, survival was prolonged in PTCy 10 (MST=36 days) (P=0.05), PTCy 25 (MST=35.5 days) (P=0.21) and PTCy 33 mice (MST=43.5 days) (P=0.03) (Figure 1E). Notably, 30% of PTCy 10 mice survived until the endpoint (day 70).

PTCy at any dose does not improve histological outcomes at endpoint

We have previously observed reduced GVHD-associated liver histopathology in humanised NSG mice treated with high-dose PTCy (33 mg/kg) [44]. However, the effects of lower doses of PTCy on histological outcomes in this model have not been assessed. Thus, histology of liver, skin, ears and lungs was performed at day 70 or the ethical endpoint to compare the effects of each PTCy dose on late-stage GVHD in humanised NSG mice (Figure 2).

Substantial immune cell infiltration and tissue damage were observed in the liver of Ctrl mice (histological grades 0.5–3, mean>1.5) (Figure 2A). Treatment with either low-, mid- or high-dose PTCy did not reduce GVHD-associated liver histopathology (histological grades 0.5–3, mean>1.5) (P=0.93). Moreover, histological evidence of GVHD was similar among all groups in the skin (histological grades 1–3, mean>2) (P=0.14) (Figure 2B) and ear (histological grades 1–4, mean>1.5) (P=0.16) (Figure 2C), with mice across all groups experiencing epidermal thickening and immune cell infiltration. The mean percentage of clear alveoli space (an inverse measure of lung GVHD) in the lungs of Ctrl mice was 30.2%, and this was similar in mice treated with each dose of PTCy (27.1–31.8%) (P=0.64) (Figure 2D).

© 2025 The Author(s). This is an open access article published by Portland Press Limited on behalf of the Biochemical Society and distributed under the Creative Commons Attribution License 4.0 (CC BY).

Clinical Science (2025) **139** 1261–1285
https://doi.org/10.1042/CS20257272

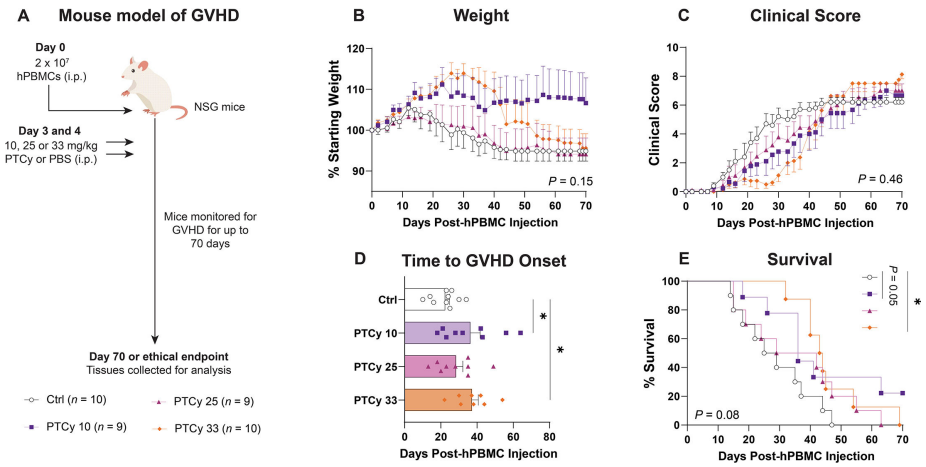


Figure 1: Low-dose PTCy prolongs time to GVHD onset in humanised NSG mice.

(A) Schematic overview of the humanised mouse model. NSG mice were injected i.p. with 2×10^7 hPBMCs (n=6 donors) and subsequently injected i.p. on days 3 and 4 post-hPBMC injection with cyclophosphamide (PTCy) at 10 mg/kg (PTCy 10), 25 mg/kg (PTCy 25) or 33 mg/kg (PTCy 33), or with PBS (Ctrl). Mice were monitored for clinical signs of GVHD, including (B) weight and (C) clinical score, over 70 days. (D) Time to GVHD onset (defined as a clinical score ≥ 3) and (E) survival were also assessed. Data are presented as the mean ± standard error of the mean (n=8–10). Data are from two independent experiments with two or six donors. Significance was analysed using (B, C) two-way ANOVA, (D) one-way ANOVA and (E) log-rank (Mantel–Cox) tests, with normality tested using a Shapiro–Wilk test. *P<0.05.

Low- and mid-dose PTCy do not affect splenic human leukocyte subsets at endpoint

High-dose PTCy (33 mg/kg) can alter the proportions of human (h) leukocytes in humanised NSG mice [44,47]; however, the impact of low- and mid-dose PTCy on human leukocyte subsets in this model is yet to be explored. Therefore, human immune cell subsets in spleens from the humanised mice above were assessed by flow cytometry (using a consistent gating strategy) (Figure 3A) at day 70 or the ethical endpoint.

PTCy at any dose did not affect engraftment of hCD45$^+$ leukocytes, with each group showing similar proportions (52.2–75.2%) compared with Ctrl mice (63.6%) (P=0.21) (Figure 3B). These cells were predominantly hCD3$^+$ T cells with similar proportions in all four groups (88.8–99.2%) (P=0.20) (Figure 3C). The splenic hCD4$^+$:hCD8$^+$ T cell ratio correlates with clinical GVHD severity in both humans [48,49] and in humanised NSG mice [46]. Proportions of hCD4$^+$ and hCD8$^+$ T cells were similar in all four groups (P=0.86) (Figure 3D), resulting in similar hCD4$^+$:hCD8$^+$ T cell ratios (1.2–2.9) (P=0.72) (Figure 3E).

Tregs can reduce GVHD severity by inhibiting the activation and proliferation of effector T cells [35,50]. PTCy at any dose did not affect the proportions of splenic hTregs (hCD4$^+$hCD25$^+$hCD127^{low}) (5.5–6.9%) compared with Ctrl mice (6.9%) (P=0.91) (Figure 3F). Proportions of highly suppressive hCD39$^+$ hTregs [51] were also similar across all groups (42.1–46.5%) (P=0.94) (Figure 3G). Notably, mice reconstituted with hPBMCs from different donors exhibited variable proportions of hCD39$^+$hTregs, with some donors resulting in markedly lower proportions in recipient mice.

Th17 cells play a pathogenic role in GVHD [52]. Compared with Ctrl mice (15.3%), proportions of splenic hTh17 cells (hCD4$^+$hCD183$^-$hCD161$^+$) were similar in PTCy 10 and PTCy 25 mice (7.7%) (P=0.30 and P=0.28, respectively). However, splenic hTh17 cells were reduced by 72% in PTCy 33 mice, which approached statistical significance (P=0.07) (Figure 3H). Compared with Ctrl mice, the hTh17:hTreg ratio was similar in PTCy-treated mice (P=0.30) (Figure 3I).

Th1 cell maturation is a dominant feature of GVHD development, with elevated Th1 cytokines correlating with greater disease severity and earlier onset in preclinical models [53,54]. Compared with Ctrl mice (27.7%), proportions of hTh1 cells (hCD4$^+$hCD183$^+$hCD161$^-$) were approximately two-fold higher in PTCy 10, PTCy 25 (P=0.11 and P=0.13, respectively) and PTCy 33 mice (59.1–51.7%), which approached statistical significance in the latter group only (P=0.05) (Figure 3J).

© 2025 The Author(s). This is an open access article published by Portland Press Limited on behalf of the Biochemical Society and distributed under the Creative Commons Attribution License 4.0 (CC BY).

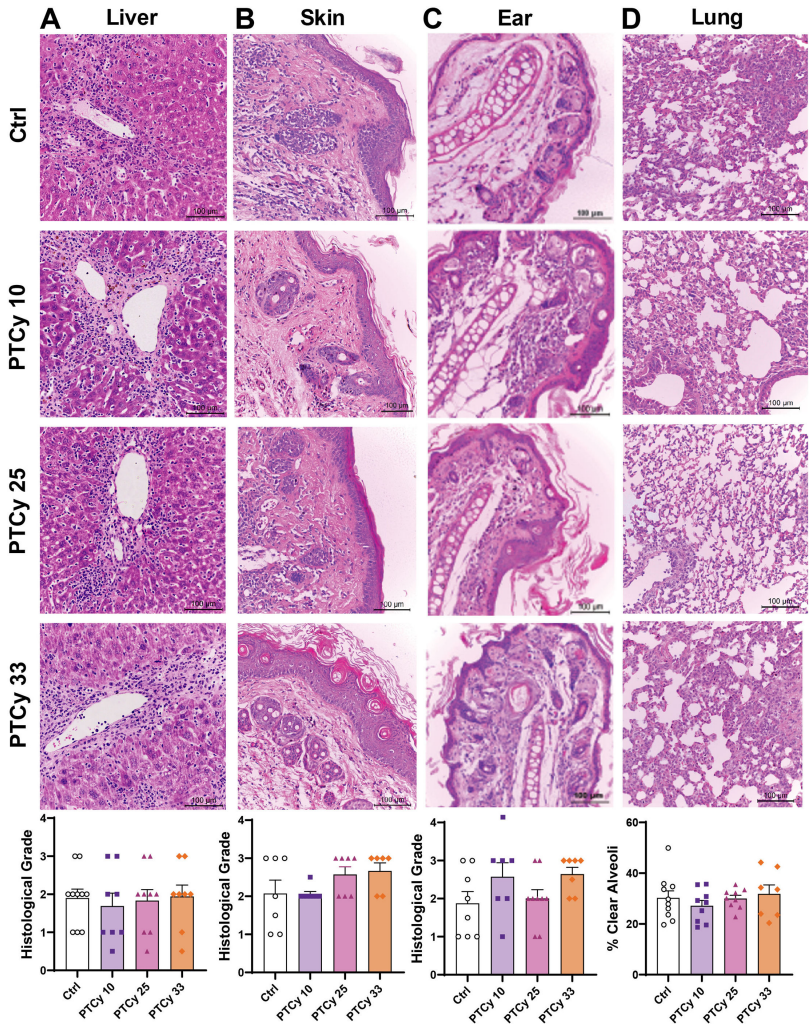


Figure 2: PTCy at any dose does not improve histological outcomes at endpoint.

At day 70 or ethical endpoint, organs were sectioned (3–5 µm) and stained with haematoxylin and eosin. Sections of (A) liver, (B) skin, (C) ear and (D) lung were examined for histological GVHD. (A-C) Liver, skin and ear were assessed using a standardised grading system and (D) lung was assessed as the percentage of clear alveoli area of total lung area. Images are representative of 7–10 mice per treatment group. Data are presented as the mean ± standard error of the mean (n=7–10). Data are from two independent experiments. Normality was assessed using a Shapiro–Wilk test and significance was analysed using (A-C) Kruskal–Wallis and (D) one-way ANOVA tests.

Cytotoxic T (Tc) 17 cells ($hCD8^+hCD161^{high}$) can induce GVHD [55]. Apart from one mouse in the PTCy 33 group, proportions of hTc17 cells were relatively low and similar across all groups (0.76–2.19%) (P=0.73) (Figure 3K).

Human killer cell immunoglobulin-like receptor $(KIR)^+CD8^+$ T cells, equivalent to mouse $Ly49^+$ $CD8^+$ Tregs, are a recently identified subset that are particularly active during infections and are thought to regulate self-reactive T cells that are activated by infection [56,57]. However, the role of these regulatory cells in GVHD is unknown. Excluding one mouse in each of the Ctrl and PTCy 10 groups, proportions of splenic $hKIR^+hCD8^+$ cells ($hCD8^+hCD158e1^+$) were similar across all groups (1.5–4.7%) (P=0.75) (Figure 3L).

$CD3^+CD56^+$ T cells are a heterogeneous population of unconventional (hUnconv) T cells, including mucosal-associated invariant T cells, γδ T cells and natural killer (NK) T cells [58]. In the context of GVHD, the role of hUnconv T cells is not fully elucidated, but their dual functionality suggests they could contribute to both the pathogenesis and regulation of GVHD [59–61]. PTCy, at any dose, did not affect proportions of hUnconv T cells ($hCD3^+hCD56^+$), with similar proportions observed in all groups (39.2–55.3%) (P=0.19) (Figure 3M).

© 2025 The Author(s). This is an open access article published by Portland Press Limited on behalf of the Biochemical Society and distributed under the Creative Commons Attribution License 4.0 (CC BY).

Clinical Science (2025) **139** 1261–1285
https://doi.org/10.1042/CS20257272

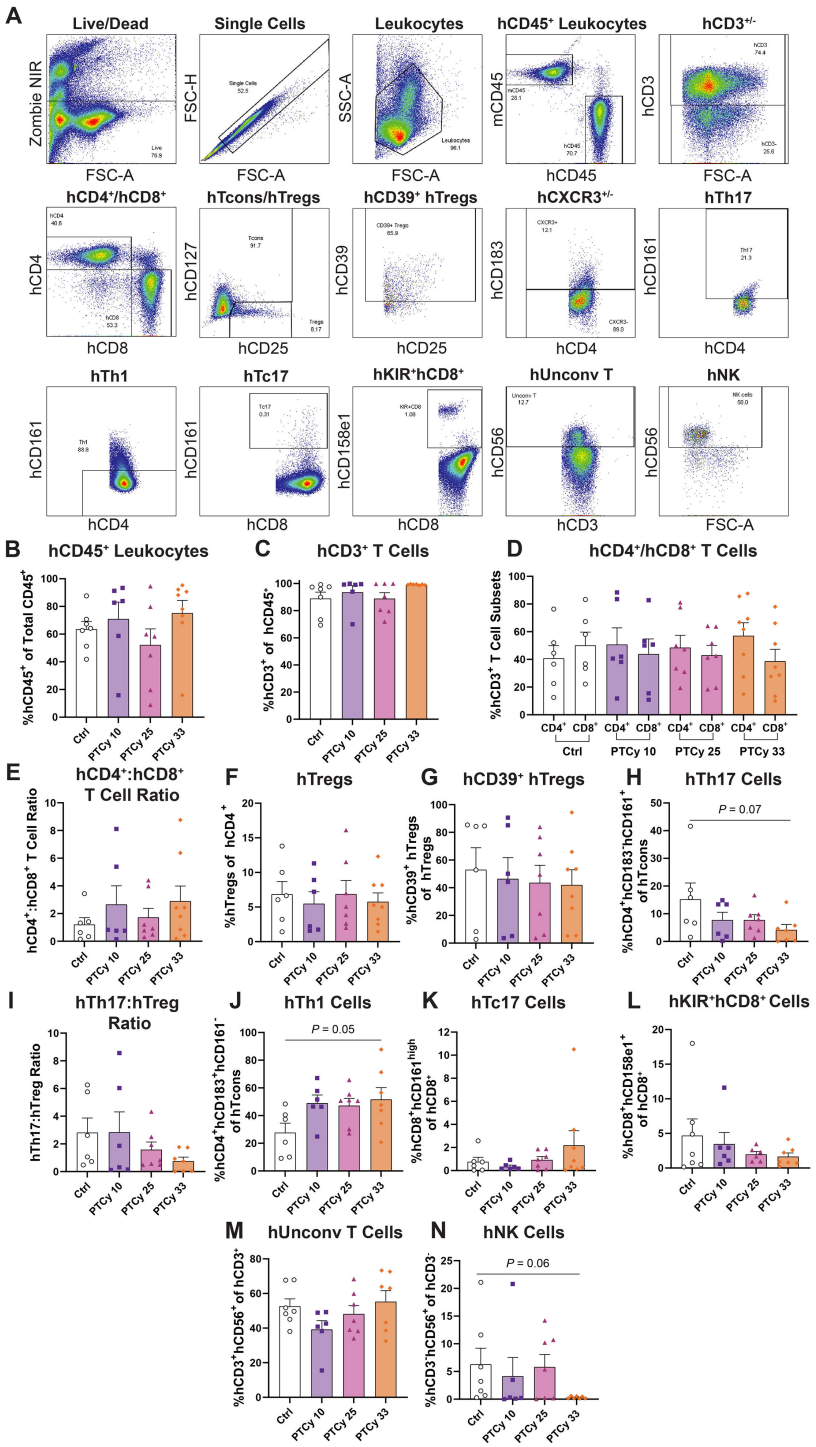


Figure 3: Low- and mid-dose PTCy do not affect splenic human leukocyte subsets at endpoint.

(A) Spleens from humanised mice were collected at day 70 or ethical endpoint and immune cell subsets were analysed by flow cytometry using a consistent gating strategy. Live cells were gated based on Zombie near infrared (NIR) staining. Single cells were gated based on forward scatter area (FSC-A) and forward scatter height (FSC-H) before viable human (h) and mouse (m) leukocytes were gated using FSC-A and side scatter area (SSC-A). hCD45$^+$ and mCD45$^+$ leukocytes were then gated before identifying hCD3$^+$ and hCD3$^-$ cells. Within the hCD3$^+$ population, hCD4$^+$ and hCD8$^+$ T cells were gated before identifying hCD25$^+$hCD127^{low} hTregs, hCD39$^+$ hTregs, hCD8$^+$hCD161^{high} hTc17 cells, hCD8$^+$hCD158e1$^+$ hKIR$^+$hCD8$^+$ cells and hCD3$^+$hCD56$^+$ hUnconventional (hUnconv) T cells. hCD183$^{+/-}$ (CXCR3) cells were gated before hCD4$^+$hCD183$^-$hCD161$^+$ hTh17 cells hCD4$^+$hCD183$^+$hCD161$^-$ hTh1 cells were identified. Within the hCD3$^-$ population, hCD3$^-$hCD56$^+$ NK cells were identified. (B) hCD45$^+$ and mCD45$^+$ leukocytes were gated before identifying (C) hCD3$^+$ T cells, (D) hCD4$^+$ and hCD8$^+$ T cell subsets, (E) hCD4$^+$:hCD8$^+$ T cell ratios, (F) hTregs, (G) hCD39$^+$ hTregs, (H) hTh17 cells, (I) hTh17:hTreg ratios, (J) hTh1 cells, (K) hTc17 cells, (L) hKIR$^+$hCD8$^+$ cells, (M) hUnconv T cells and (N) hNK cells. Data are presented as the mean ± standard error of the mean (n=6–8). Symbols represent individual mice. Data are from two independent experiments. Normality was assessed using a Shapiro–Wilk test and significance was tested using (D, F, H, I, J, M) one-way ANOVA or (B, C, E, G, K, L, N) Kruskal–Wallis tests.

© 2025 The Author(s). This is an open access article published by Portland Press Limited on behalf of the Biochemical Society and distributed under the Creative Commons Attribution License 4.0 (CC BY).

NK cells are the primary human non-T cell population to engraft in this model [62] and can suppress GVHD in mice while promoting GVL immunity [63]. Compared with Ctrl mice, proportions of hNK cells ($hCD3^{-}hCD56^{+}$) were similar in PTCy 10 and PTCy 25 mice (4.2–6.3%) (P=0.32 and P>0.99, respectively) but were reduced by 95.2% in PTCy 33 mice, which approached statistical significance (P=0.06) (Figure 3N).

PTCy at any dose does not affect hepatic human leukocyte subsets at endpoint

The liver is a primary target organ of GVHD in both humans [64] and humanised NSG mice [65]. Therefore, human immune cell subsets in livers from the humanised mice above were assessed by flow cytometry (using a consistent gating strategy) (Figure 3A) at day 70 or the ethical endpoint.

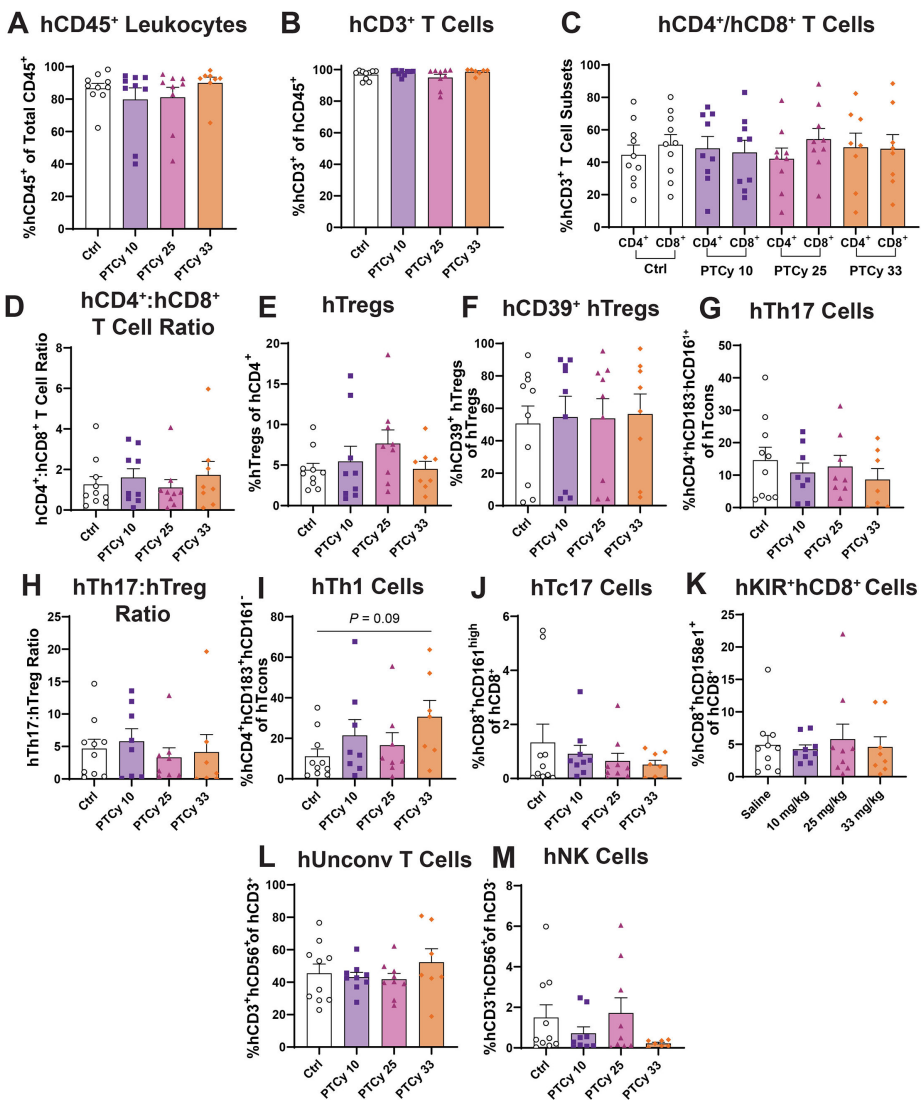


Figure 4: PTCy at any dose does not affect hepatic human leukocyte subsets at endpoint.

Livers from humanised mice were collected at day 70 or the ethical endpoint, and immune cell subsets were analysed by flow cytometry using the gating strategy shown in **Figure 3A** (A) $hCD45^{+}$ and $mCD45^{+}$ leukocytes were gated before identifying (B) $hCD3^{+}$ T cells, (C) $hCD4^{+}$ and $hCD8^{+}$ T cell subsets, (D) $hCD4^{+}$:$hCD8^{+}$ T cell ratios, (E) hTregs, (F) $hCD39^{+}$ hTregs, (G) hTh17 cells, (H) hTh17:hTreg ratios, (I) hTh1 cells, (J) hTc17 cells, (K) $hKIR^{+}hCD8^{+}$ cells, (L) hUnconv T cells and (M) hNK cells. Data are presented as the mean ± standard error of the mean (n=7–10). Symbols represent individual mice. Data are from two independent experiments. Normality was assessed using a Shapiro–Wilk test and significance was tested using (C, L) one-way ANOVA or (A, B, D, E, F, G, H, I, J, K, M) Kruskal–Wallis tests.

© 2025 The Author(s). This is an open access article published by Portland Press Limited on behalf of the Biochemical Society and distributed under the Creative Commons Attribution License 4.0 (CC BY).

Clinical Science (2025) **139** 1261–1285
https://doi.org/10.1042/CS20257272

As observed in the spleen (Figure 3), PTCy at any dose did not affect proportions of hCD45$^+$ leukocytes in the liver, with all groups showing similar proportions to Ctrl mice (79.8–90.0%) (P=0.36) (Figure 4A). These cells were predominantly hCD3$^+$ T cells, with similar proportions in all four groups (94.9–98.6%) (P=0.20) (Figure 4B). Furthermore, proportions of hCD4$^+$ and hCD8$^+$ T cells were similar in all four groups (P=0.96) (Figure 4C), as were the hCD4$^+$:hCD8$^+$ T cell ratios (1.1–1.7) (P=0.92) (Figure 4D).

In the liver, PTCy at any dose did not affect proportions of hTregs with similar proportions in PTCy-treated (4.5–7.7%) and Ctrl mice (4.4%) (P=0.33) (Figure 4E). Furthermore, proportions of hCD39$^+$ Tregs were also similar across all four groups (50.6–56.4%) (P=0.89), again with notable variation related to donors used (Figure 4F).

Proportions of hepatic hTh17 cells were similar between Ctrl (14.6%) and PTCy-treated mice (8.6–10.8%) (P=0.68) (Figure 4G), as were hTh17:hTreg ratios (3.3–5.8) (P=0.65) (Figure 4H). Compared with Ctrl mice (11.1%), proportions of hepatic hTh1 cells were similar in PTCy 10 (21.4%) and PTCy 25 (16.6%) mice (P=0.75 and P>0.99, respectively) but were increased approximately three-fold in PTCy 33 (30.6%) mice, which approached statistical significance (P=0.09) (Figure 4I).

Apart from two mice in the Ctrl group, proportions of hTc17 cells were low (0.5–1.3%) and similar in all four groups (P=0.62) (Figure 4J). Compared with Ctrl mice (4.9%), proportions of hKIR$^+$hCD8$^+$ cells were similar in PTCy-treated groups (4.2–5.8%) (P=0.94) (Figure 4K).

Compared with Ctrl mice (45.4%), proportions of hUnconv T cells were similar in PTCy-treated groups (41.8–52.3%) (P=0.56) (Figure 4L). Proportions of hNK cells were similar between Ctrl (1.5%) and PTCy-treated mice (0.2–1.7%) (P=0.56) (Figure 4M).

PTCy doses differentially affect splenic human PD-1$^+$ T cell subsets at endpoint

The precise mechanisms through which PTCy reduces GVHD remain incompletely understood. Previous studies have indicated that PTCy may work via the induction of effector T cell dysfunction or exhaustion [19,66], but there is limited data investigating this notion. As such, the effects of low-, mid- and high-dose PTCy on splenic T cell subsets expressing co-inhibitory receptors PD-1 and LAG3, which are known markers for exhausted T cells [27,29], were assessed by flow cytometry at day 70 or the ethical endpoint. These markers were assessed using the above gating strategy (as shown in Figure 3A) before identifying hPD-1$^+$ and hLAG3$^+$ cells using a consistent gating strategy (Figure 5A).

Compared with Ctrl mice (30.4%), proportions of splenic hPD-1$^+$hCD4$^+$ T cells were significantly increased 1.7-fold in low-dose PTCy 10 mice (P=0.03) but were similar in PTCy 25 (P=0.21) and PTCy 33 mice (P=0.48) (Figure 5B). Compared with Ctrl mice (24.5%), proportions of splenic hPD-1$^+$hCD8$^+$ T cells were also significantly increased 1.9-fold in PTCy 10 mice (P=0.03) but were similar in PTCy 25 (P=0.21) and PTCy 33 mice (P=0.29) (Figure 5C). In contrast, compared with Ctrl mice (23.1%), proportions of splenic hPD-1$^+$hTregs were significantly increased by 2.1-fold in PTCy 10 (P=0.004), 2.4-fold in PTCy 25 (P=0.0006) and 1.7-fold in PTCy 33 mice (P=0.04) (Figure 5D).

Compared with Ctrl mice (10.1%), proportions of splenic hLAG3$^+$hCD4$^+$ T cells were similar in PTCy-treated mice (P=0.18) (Figure 5E). Similarly, compared with Ctrl mice (22.1%), proportions of splenic hLAG3$^+$hCD8$^+$ T cells were similar in PTCy-treated mice (P=0.29) (Figure 5F). Proportions of hLAG3$^+$hTregs were similar in PTCy 10 (P=0.12) and PTCy 33 mice (P=0.18) but were significantly reduced by 78.1% in PTCy 25 mice (P=0.02) compared with Ctrl mice (17.3%) (Figure 5G).

Proportions of splenic hPD-1$^+$hLAG3$^+$hCD4$^+$ T cells were similar in Ctrl (12.2%) and PTCy-treated mice (1.3–4.9%) (P=0.15) (Figure 5H). Markedly, compared with Ctrl mice (16.4%), proportions of splenic hPD-1$^+$hLAG3$^+$hCD8$^+$ T cells were similar in PTCy 10 (18.5%) and PTCy 25 mice (14.1%) (P=0.99 and P=0.98, respectively), but were significantly increased 2.1-fold in PTCy 33 mice (34.5%) (P=0.04) (Figure 5I). Proportions of splenic hPD-1$^+$hLAG3$^+$hTregs were similar across all four groups (16.5–32.1%) (P=0.65) (Figure 5J).

PTCy doses do not differentially affect hepatic human PD-1$^+$ T cell subsets at endpoint

In the liver, proportions of hPD-1$^+$hCD4$^+$ T cells were similar between Ctrl and low-, mid- and high-dose PTCy-treated mice (53.9–65.0%) (P=0.31) (Figure 6A), as were proportions of hPD-1$^+$hCD8$^+$ T cells (48.6–59.9%) (P=0.28) (Figure 6B). Furthermore, proportions of hPD-1$^+$hTregs were similar between all four

© 2025 The Author(s). This is an open access article published by Portland Press Limited on behalf of the Biochemical Society and distributed under the Creative Commons Attribution License 4.0 (CC BY).

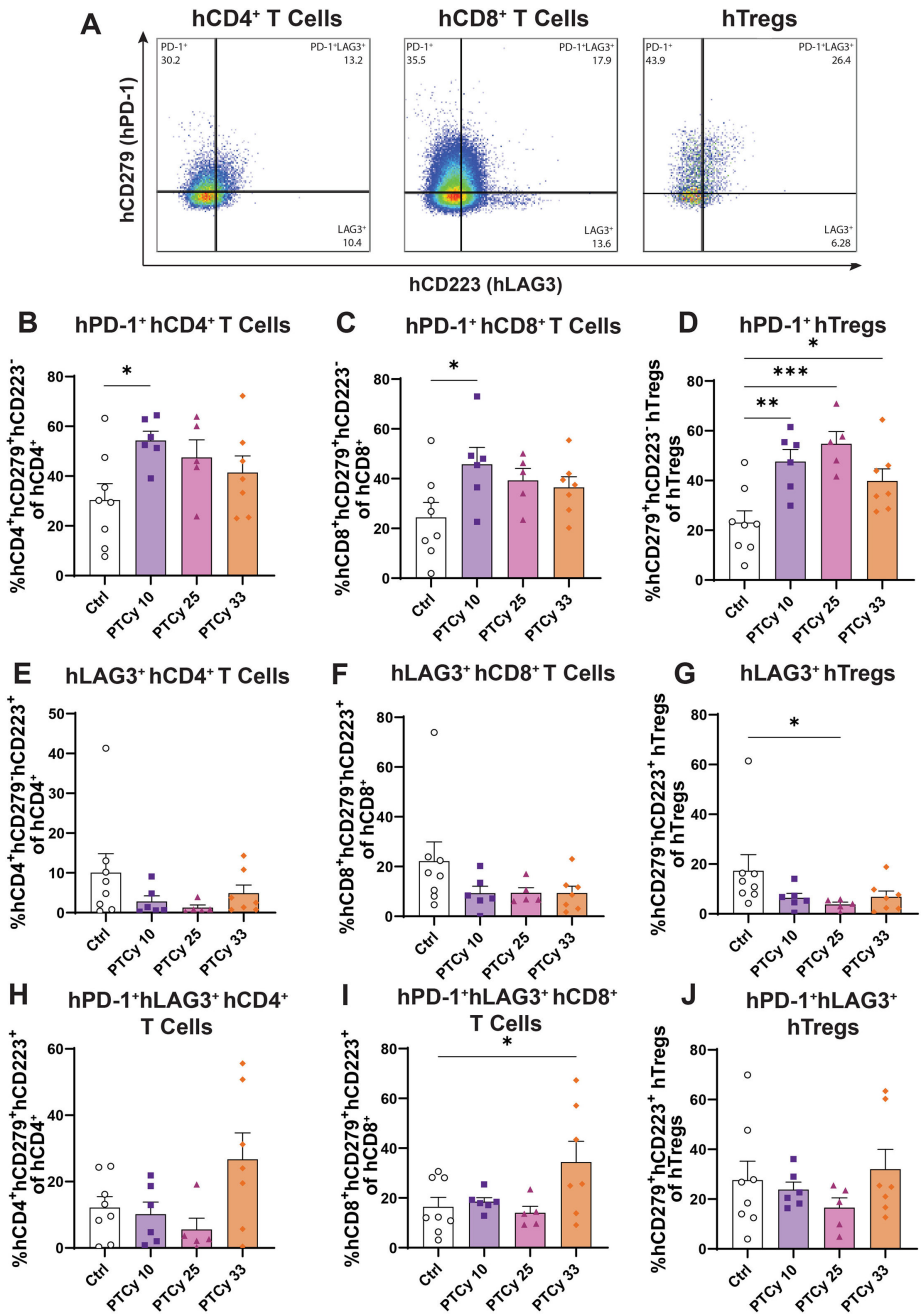


Figure 5: PTCy doses differentially affect splenic human PD-1⁺ T cell subsets at endpoint.

Spleens from humanised mice were collected at day 70 or ethical endpoint and were examined by flow cytometry. Proportions of human (H) CD45⁺ leukocytes, hCD3⁺ T cells, hCD4⁺ and hCD8⁺ T cell subsets and hTregs were identified using the gating strategy shown in Figure 3A before assessing (A) hCD279⁺hCD223⁻ (hPD-1⁺), hCD279⁻hCD223⁺ (hLAG3⁺) and hCD279⁺hCD223⁺ (hPD-1⁺hLAG3⁺) subsets as shown. Proportions of (B) hPD-1⁺hCD4⁺ T cells, (C) hPD-1⁺hCD8⁺ T cells, (D) hPD-1⁺hTregs, (E) hLAG3⁺hCD4⁺ T cells, (F) hLAG3⁺hCD8⁺ T cells, (G) hLAG3⁺hTregs, (H) hPD-1⁺hLAG3⁺hCD4⁺ T cells, (I) hPD-1⁺hLAG3⁺hCD8⁺ T cells and (J) hPD-1⁺hLAG3⁺hTregs were assessed. Data are presented as the mean ± standard error of the mean (n=5–8). Data are from two independent experiments. Normality was assessed using a Shapiro–Wilk test and significance was tested using (B, C, D, I) one-way ANOVA or (E, F, G, H, J) Kruskal–Wallis tests. ***P<0.001, **P<0.01, *P<0.05.

groups (50.6–60.2%) (P=0.38) (Figure 6C). Moreover, proportions of hepatic hLAG3⁺hCD4⁺ T cells were relatively low and similar between Ctrl and PTCy-treated mice (1.9–3.3%) (P=0.83) (Figure 6D), as were proportions of hLAG3⁺hCD8⁺ T cells (3.8–6.2%) (P=0.98) (Figure 6E) and proportions of hLAG3⁺hTregs (2.8–5.4%) (P=0.28) (Figure 6F).

In the liver, proportions of hPD-1⁺hLAG3⁺hCD4⁺ T cells were similar in Ctrl (11.1%) and PTCy-treated mice (10.0–22.4%) (P=0.10) (Figure 6G). Like the spleen, hepatic proportions of hPD-1⁺hLAG3⁺hCD8⁺

© 2025 The Author(s). This is an open access article published by Portland Press Limited on behalf of the Biochemical Society and distributed under the Creative Commons Attribution License 4.0 (CC BY).

Clinical Science (2025) **139** 1261–1285
https://doi.org/10.1042/CS20257272

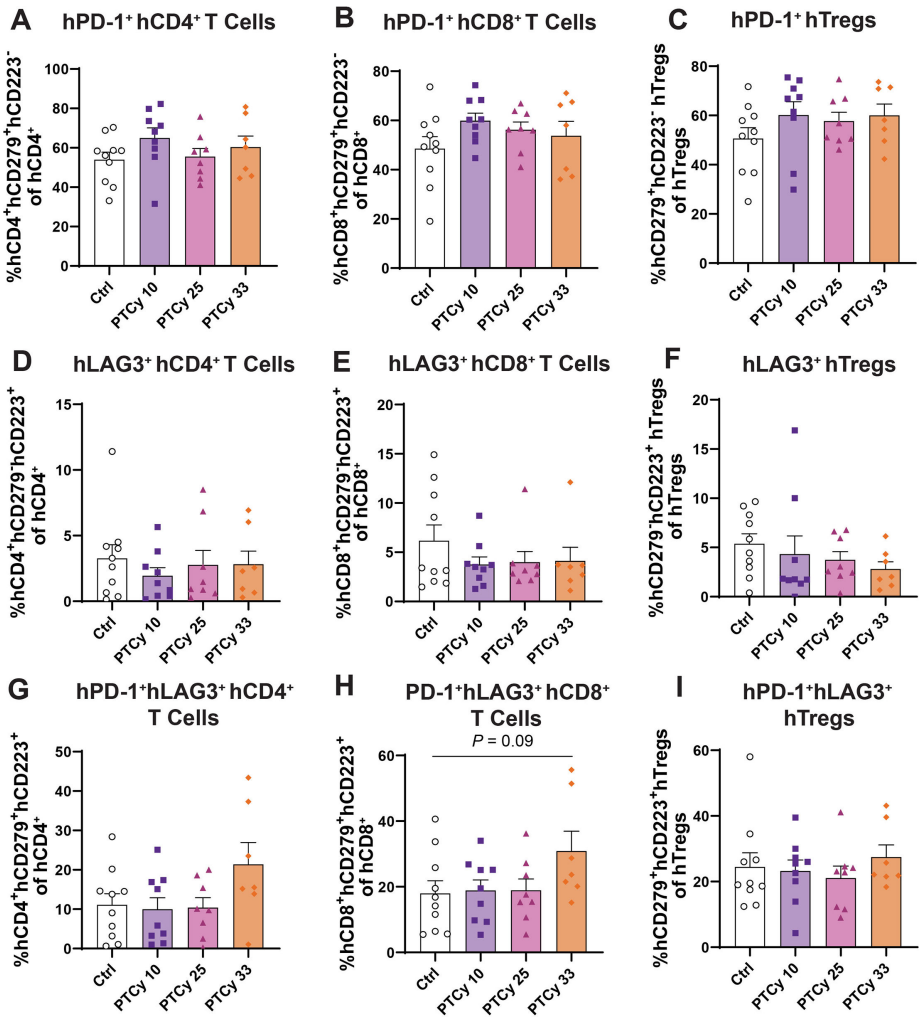


Figure 6: PTCy doses do not differentially affect hepatic human PD-1⁺ T cell subsets at endpoint.

Livers from humanised mice were collected at day 70 or the ethical endpoint and were examined by flow cytometry. Proportions of human (h) CD45⁺ leukocytes, hCD3⁺ T cells, hCD4⁺ and hCD8⁺ T cell subsets and hTregs were identified using the gating strategy shown in Figure 3A before assessing hCD279⁺hCD223⁻ (hPD-1⁺), hCD279⁻hCD223⁺ (hLAG3⁺) and hCD279⁺hCD223⁺ (hPD-1⁺hLAG3⁺) subsets as shown in Figure 5A. Proportions of (A) hPD-1⁺hCD4⁺ T cells, (B) hPD-1⁺hCD8⁺ T cells, (C) hPD-1⁺hTregs, (D) hLAG3⁺hCD4⁺ T cells, (E) hLAG3⁺hCD8⁺ T cells, (F) hLAG3⁺hTregs, (G) hPD-1⁺hLAG3⁺hCD4⁺ T cells, (H) hPD-1⁺hLAG3⁺hCD8⁺ T cells and (I) hPD-1⁺hLAG3⁺hTregs were assessed. Data are presented as the mean ± standard error of the mean (n=7–10). Data are from two independent experiments. Normality was assessed using a Shapiro–Wilk test and significance was tested using (A, B, G, H) one-way ANOVA or (C, D, E, F, I) Kruskal–Wallis tests.

T cells were similar in Ctrl, PTCy 10 and PTCy 25 mice (18.0–18.9%) (P=0.99 and P=0.99, respectively), but were increased 1.7-fold in PTCy 33 mice (30.9%), which approached statistical significance (P=0.09) (Figure 6H). Proportions of hPD-1⁺hLAG3⁺hTregs were similar between Ctrl and low-, mid- and high-dose PTCy-treated mice (21.1–27.5%) (P=0.73) (Figure 6I).

Low-dose PTCy does not improve clinical signs of GVHD early in disease

To better understand the mechanisms by which PTCy attenuates GVHD, NSG mice were injected i.p. with hPBMCs (from four healthy donors) and with low, mid or high doses of PTCy or PBS as above (Figure 1) but were euthanised at day 28 during the early stages of GVHD development (Figure 7A).

Weight loss was observed in Ctrl mice from day 18, whereas low-, mid- and high-dose PTCy-treated mice gained and maintained weight until day 28 (Figure 7B). However, the overall difference in weight between groups was not statistically significant (P=0.94).

© 2025 The Author(s). This is an open access article published by Portland Press Limited on behalf of the Biochemical Society and distributed under the Creative Commons Attribution License 4.0 (CC BY).

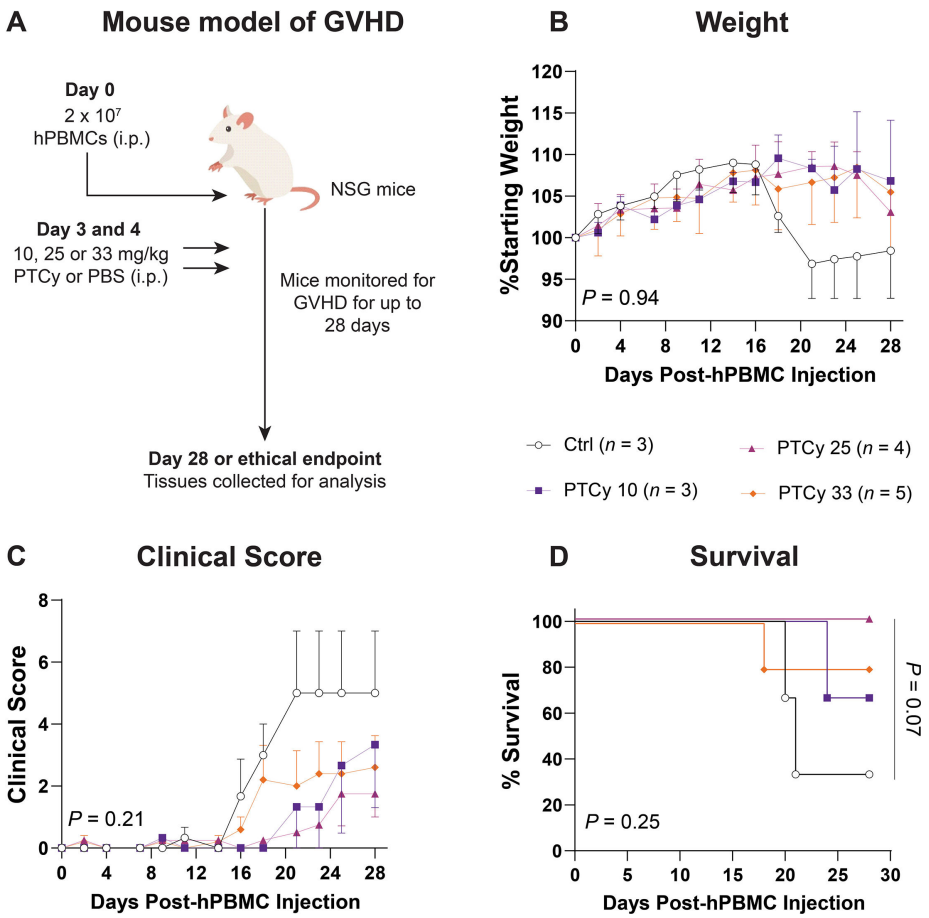


Figure 7: PTCy at any dose does not improve clinical signs of GVHD early in disease.

(A) Schematic overview of the humanised mouse model. NSG mice were injected i.p. with 2×10^7 hPBMCs (n=4 donors) and subsequently injected i.p. on days 3 and 4 post-hPBMC injection with cyclophosphamide (PTCy) at 10 mg/kg (PTCy 10), 25 mg/kg (PTCy 25) or 33 mg/kg (PTCy 33) or with PBS (Ctrl). Mice were monitored for clinical signs of GVHD, including (B) weight, (C) clinical score and (D) survival over 28 days. Data are presented as the mean ± standard error of the mean (n=3–5). Data are from one experiment. Significance was analysed using (B, C) two-way ANOVA and (D) log-rank (Mantel–Cox) tests.

Clinical scores of Ctrl mice increased from day 16 before plateauing from day 20 (Figure 7C). Clinical scores of PTCy 33 mice also increased from day 16, but to a lesser extent than Ctrl mice, plateauing from day 18. Clinical scores of PTCy 10 and PTCy 25 mice increased from day 21. However, there was no statistically significant difference between groups (P=0.21).

Compared with Ctrl mice (MST=21 days), survival was prolonged in PTCy 10 (MST>28 days) (P=0.30), PTCy 25 (MST>28 days) (P=0.07) and PTCy 33 mice (MST>28 days) (P=0.30) (Figure 7D).

Low- and high-dose PTCy partially improve histological liver GVHD early in disease

Reduced liver histopathology has previously been observed following treatment with high-dose PTCy (33 mg/kg) at day 28 [47], but the effects of low- and mid-dose PTCy on histological GVHD in this model are yet to be explored. Therefore, histology of liver, skin, ears and lungs was performed at day 28 to examine the effects of low- and mid-dose PTCy on early GVHD in humanised NSG mice (Figure 8).

Moderate immune cell infiltration was observed in the liver of Ctrl mice (histological grades 1–2, mean=1.7) (Figure 8A). Compared with Ctrl mice, liver histopathology was reduced in PTCy 10 and PTCy 33 mice (histological grades 0.5–1, mean<1) with values approaching statistical significance (P=0.09 and P=0.07, respectively), but was similar in PTCy 25 mice (histological grades 1–2, mean=1.3) (P>0.99). Histological evidence of GVHD in the skin (histological grades 1–2, mean<1) (Figure 8B) and ear

© 2025 The Author(s). This is an open access article published by Portland Press Limited on behalf of the Biochemical Society and distributed under the Creative Commons Attribution License 4.0 (CC BY).

Clinical Science (2025) **139** 1261–1285
https://doi.org/10.1042/CS20257272

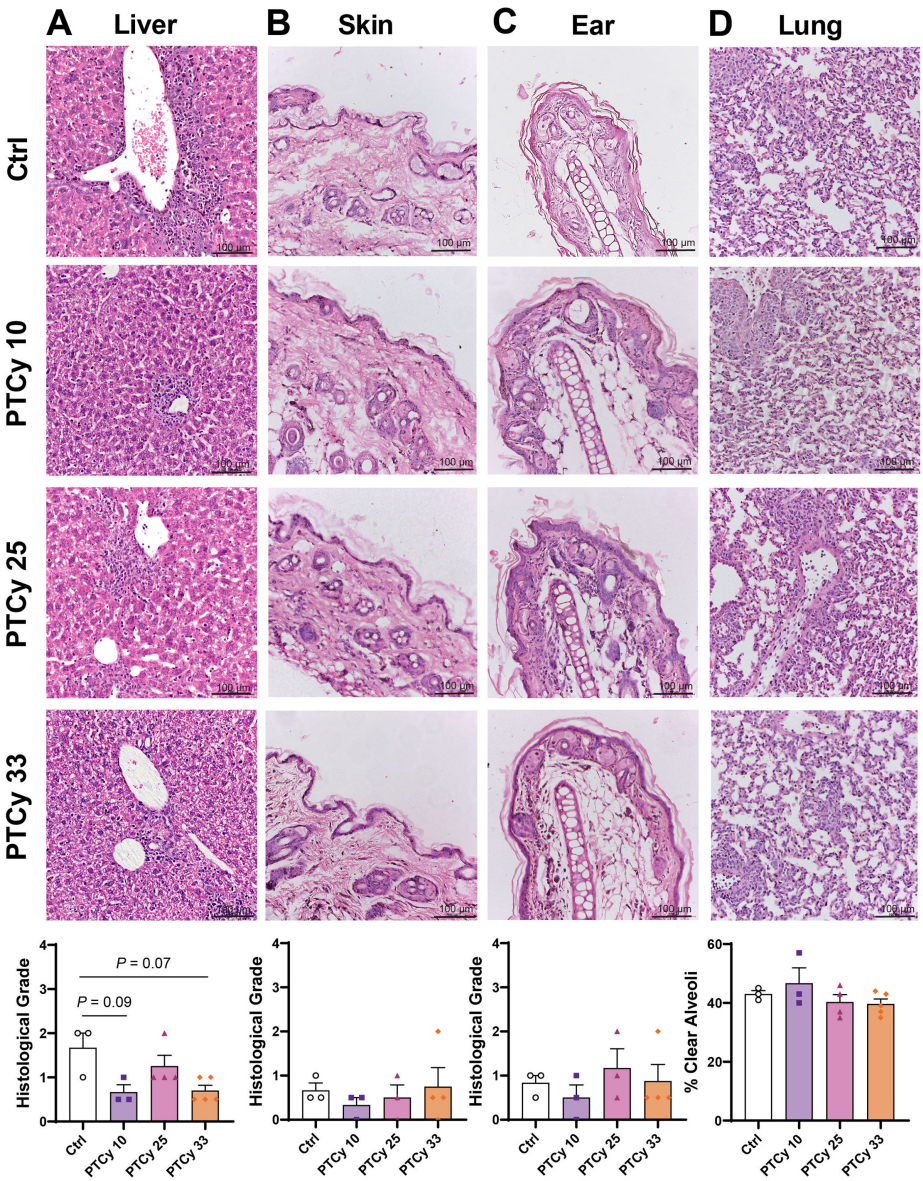


Figure 8: Low- and high-dose PTCy partially improve histological liver GVHD early in disease.

At day 28 or the ethical endpoint, organs were sectioned (3–5 µm) and stained with haematoxylin and eosin. Sections of (A) liver, (B) skin, (C) ear and (D) lung were examined for histological GVHD. (A-C) Liver, skin and ear were assessed using a standardised grading system and (D) lung was assessed as the percentage of clear alveoli area of total lung area. Images are representative of 3–5 mice per treatment group. Data are presented as the mean ± standard error of the mean (n=3–5). Data are from one experiment. Normality was assessed using a Shapiro–Wilk test and significance was analysed using (B, D) one-way ANOVA or (A, C) Kruskal–Wallis tests.

(histological grades 0–2, mean<2) (Figure 8C) was low and similar between Ctrl and PTCy-treated mice (P=0.80 and P=0.65, respectively), with negligible evidence of epidermal thickening and low to moderate immune cell infiltration across all groups. The mean percentages of clear alveoli space in the lungs of Ctrl mice (43.0%) and in mice treated with low-, mid- or high-PTCy doses (39.6–46.7%) were similar (P=0.33) (Figure 8D).

© 2025 The Author(s). This is an open access article published by Portland Press Limited on behalf of the Biochemical Society and distributed under the Creative Commons Attribution License 4.0 (CC BY).

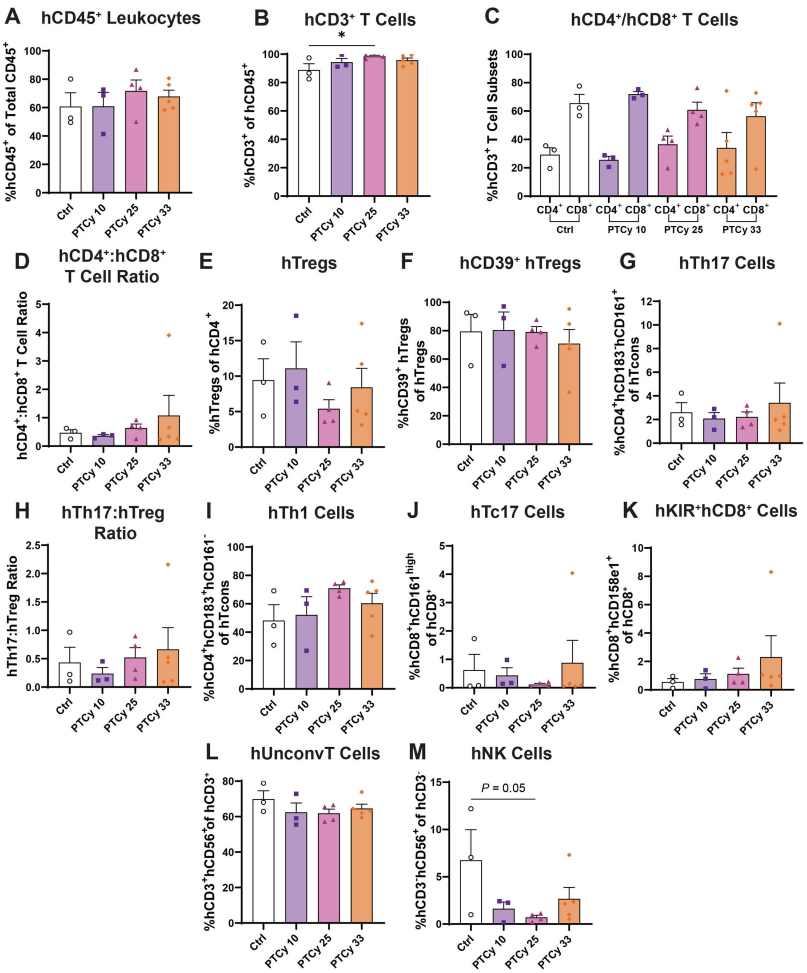


Figure 9: Mid-dose PTCy increases proportions of splenic human T cells early in disease.

Spleens from humanised mice were examined by flow cytometry using the gating strategy shown in Figure 3A to identify human (H) leukocyte subsets at day 28 or the ethical endpoint. (A) hCD45$^+$ and mCD45$^+$ leukocytes were gated before identifying (B) hCD3$^+$ T cells, (C) hCD4$^+$ and hCD8$^+$ T cell subsets, (D) hCD4$^+$:hCD8$^+$ T cell ratios, (E) hTregs, (F) hCD39$^+$ hTregs, (G) hTh17 cells, (H) hTh17:hTreg ratios, (I) hTh1 cells, (J) hTc17 cells, (K) hKIR$^+$hCD8$^+$ cells, (L) hUunconv T cells and (M) hNK cells. Data are presented as the mean ± standard error of the mean (n=3–5). Symbols represent individual mice. Data are from one experiment. Normality was assessed using a Shapiro–Wilk test and significance was tested using (A, B, E, F, I, L, M) one-way ANOVA or (C, D, G, H, J, K) Kruskal–Wallis tests. *P<0.05.

Mid-dose PTCy increases proportions of splenic human T cells early in disease

To better understand the cellular mechanisms of action by which PTCy attenuates GVHD, the effects of low-, mid- and high-dose PTCy on human leukocyte engraftment in spleens from humanised mice was assessed by flow cytometry, (as shown in Figure 3A) at day 28 or at ethical endpoint.

In the spleen, PTCy at low, mid or high doses did not affect engraftment of hCD45$^+$ leukocytes, with each group showing similar proportions compared with Ctrl mice (60.7–71.7%) (P=0.67) (Figure 9A). Proportions of hCD3$^+$ T cells were similar between Ctrl (88.8%), PTCy 10 (94.4%) (P=0.32) and PTCy 33 mice (95.7%) (P=0.13) but were significantly increased by 1.2-fold in PTCy 25 mice (98.5%) compared with Ctrl mice (P=0.03) (Figure 9B).

In both Ctrl and low-, mid- or high-dose PTCy-treated mice, splenic proportions of hCD4$^+$ T cells (25.5–36.5%) were lower than hCD8$^+$ T cells (56.3–71.9%) which were similar across all groups (P>0.99) (Figure 9C), as were the splenic hCD4$^+$:hCD8$^+$ T cell ratios (0.36–1.1) (P=0.59) (Figure 9D). PTCy at any dose did not affect splenic proportions of hTregs with similar proportions in PTCy-treated (5.4–11.1%) and Ctrl mice (9.4%) (P=0.55) (Figure 9E). Furthermore, proportions of hCD39$^+$ Tregs were similar across all four groups (70.8–80.4%) (P=0.87) (Figure 9F).

© 2025 The Author(s). This is an open access article published by Portland Press Limited on behalf of the Biochemical Society and distributed under the Creative Commons Attribution License 4.0 (CC BY).

Clinical Science (2025) **139** 1261–1285
https://doi.org/10.1042/CS20257272

At day 28, proportions of splenic hTh17 cells were relatively low and similar between Ctrl (2.6%) and PTCy-treated mice (2.1–3.4%) (P=0.99) (Figure 9G) as were hTh17:hTreg ratios (0.24–0.66) (P=0.82) (Figure 9H). Moreover, proportions of hTh1 cells were similar between Ctrl (48.1%) and PTCy-treated mice (52.1–70.9%) (P=0.30) (Figure 9I). Proportions of splenic hTc17 cells were near-absent and similar between Ctrl and PTCy-treated mice (0.1–0.8%) (P=0.63) (Figure 9J). Moreover, apart from one mouse in the PTCy 33 group, proportions of splenic hKIR$^+$hCD8$^+$ cells were relatively low and similar between control (0.54%) and PTCy-treated mice (0.75–2.3%) (P=0.70) (Figure 9K).

Splenic proportions of hUnconv T cells were similar between Ctrl (69.9%) and low-, mid- or high-dose PTCy-treated mice (61.8–64.6%) (P=0.44) (Figure 9L). Compared with Ctrl mice (6.7%), proportions of splenic hNK cells were similar in PTCy 10 (P=0.13) and PTCy 33 mice (P=0.19) but reduced by 89.4% in PTCy 25 mice (P=0.05), which approached statistical significance, noting a high degree of variation in hNK cell proportions in the control group (Figure 9M).

At day 28, the effects of PTCy at low-, mid- or high-doses on splenic hCD4$^+$ T cells, hCD8$^+$ T cells and hTregs expressing co-inhibitory receptors PD-1 and LAG3 were examined. PTCy at any dose did not affect splenic proportions of these subsets (Supplementary Figure S1).

Low-dose PTCy reduces proportions of hepatic hUnconv T cells early in disease

In the liver at day 28, PTCy at any dose did not affect engraftment of hCD45$^+$ leukocytes, with each group showing similar proportions (87.5–91.6%) compared with Ctrl mice (84.6%) (P=0.42) (Figure 10A). Proportions of hCD3$^+$ T cells were also similar between Ctrl (95.3%) and PTCy-treated mice (97.9–99.0%) (P=0.13) (Figure 10B).

In both Ctrl and PTCy-treated mice, proportions of hCD4$^+$ T cells (29.9–43.0%) were lower than hCD8$^+$ T cells (53.8–66.9%), with the difference between T cell subset proportions approaching statistical significance in PTCy 10 mice (P=0.07), but not other groups (Figure 10C). Nevertheless, hepatic hCD4$^+$:hCD8$^+$ T cell ratios were similar in all four groups (0.5–1.2) (P=0.48) (Figure 10D). Compared with Ctrl mice, hepatic proportions of hTregs were not impacted in PTCy 10, PTCy 25 or PTCy 33 mice, with similar proportions in all groups (5.3–8.5%) (P=0.63) (Figure 10E). Furthermore, proportions of hCD39$^+$ Tregs were similar across all four groups (80.8–84.8%) (P=0.96) (Figure 10F).

Proportions of hepatic hTh17 cells were low and similar in Ctrl (3.7%) and PTCy-treated mice (3.2–4.9%) (P=0.86) (Figure 10G), as were hTh17:hTreg ratios (0.5–1.0) (P=0.75) (Figure 10H). Moreover, proportions of hepatic hTh1 cells were similar between Ctrl (41.3%) and PTCy-treated mice (45.7–53.7%) (P=0.63) (Figure 10I). Apart from one mouse in the Ctrl group, proportions of hepatic hTc17 cells were near-absent and similar between Ctrl (1.0%) and PTCy-treated mice (0.2–0.6%) (P=0.36) (Figure 10J) and proportions of hepatic hKIR$^+$hCD8$^+$ cells were also low and similar between Ctrl (2.4%) and PTCy-treated mice (1.2–1.3%) (P=0.56) (Figure 10K).

Compared with Ctrl mice (61.8%), hepatic proportions of hUnconv T cells were significantly reduced by 22% in PTCy 10 mice (P=0.03) but were similar in both PTCy 25 (53.4%) and PTCy 33 mice (56.7%) (P=0.17 and P=0.48, respectively) (Figure 10L). Moreover, proportions of hepatic hNK cells were reduced by 82% in PTCy 10 (P=0.07), by 84% in PTCy 25 (P=0.049) and by 73% in PTCy 33 mice (P=0.08) compared with Ctrl mice, with PTCy 10 and PTCy 33 groups approaching statistical significance, noting a high degree of variation in the Ctrl group (Figure 10M).

At day 28, the effects of PTCy at low, mid or high doses on hepatic hCD4$^+$ T cells, hCD8$^+$ T cells and hTregs expressing co-inhibitory receptors PD-1 and LAG3 were examined. Other than a trending 1.3-fold increase in hPD-1$^+$hTregs in PTCy 25 mice, PTCy at any dose did not affect hepatic proportions of these subsets (Supplementary Figure S2).

Discussion

This study investigated whether lower doses of PTCy (10 mg/kg and 25 mg/kg) are equally as efficacious as high-dose PTCy (33 mg/kg) in limiting GVHD and assessed the effects of these different PTCy doses on human immune cell subsets and T cell exhaustion at early and late disease time points in a preclinical humanised mouse model. Findings from this study revealed that low-dose PTCy (10 mg/kg), but not mid-dose PTCy (25 mg/kg), can mitigate clinical signs of GVHD with comparable efficacy to that of high-dose PTCy (33 mg/kg), with delayed disease onset and improved survival observed in both

© 2025 The Author(s). This is an open access article published by Portland Press Limited on behalf of the Biochemical Society and distributed under the Creative Commons Attribution License 4.0 (CC BY).

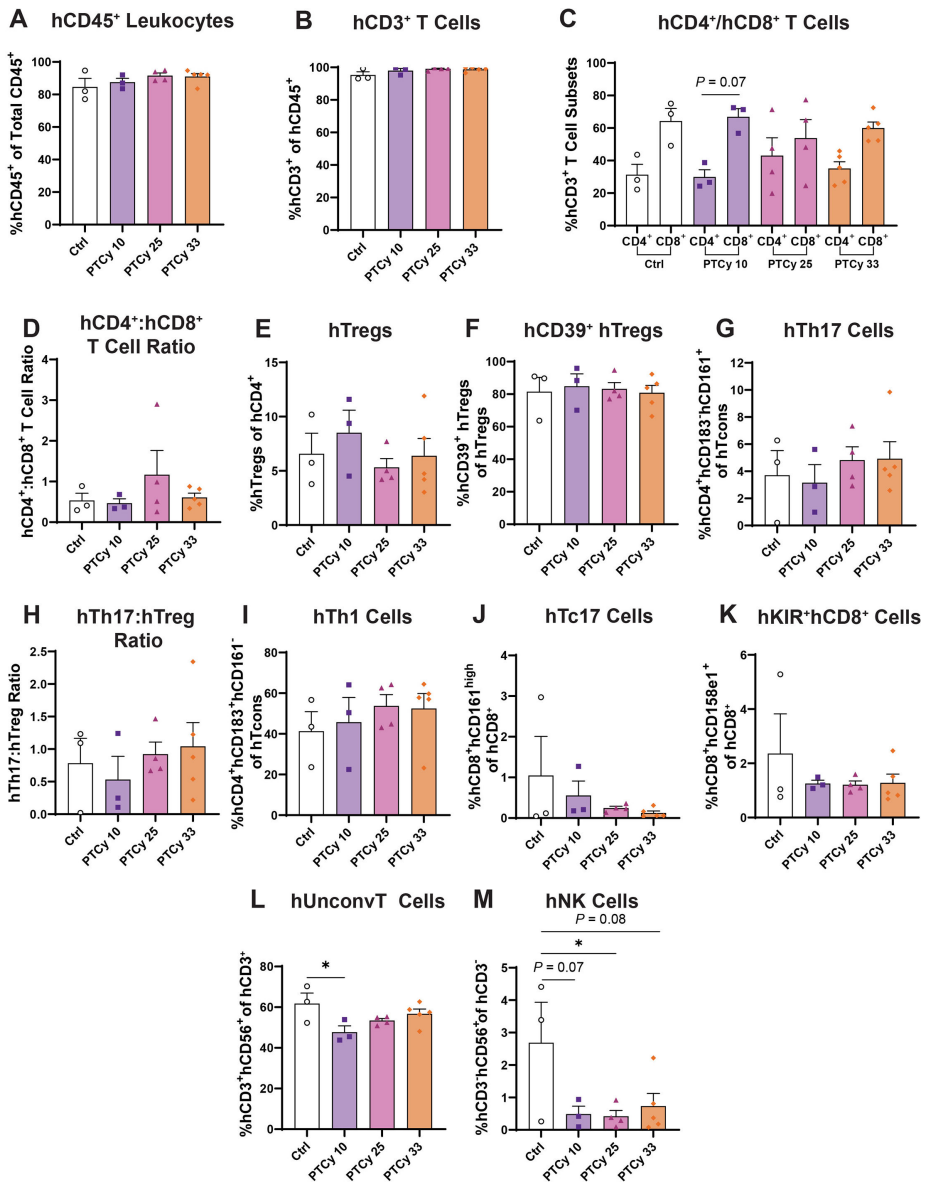


Figure 10: Low-dose PTCy reduces proportions of hepatic human UncovT cells early in disease.

Livers from humanised mice were examined by flow cytometry using the gating strategy shown in Figure 3A to identify human (h) leukocyte subsets at day 28 or the ethical endpoint. (A) hCD45$^+$ and mCD45$^+$ leukocytes were gated before identifying (B) hCD3$^+$ T cells, (C) hCD4$^+$ and hCD8$^+$ T cell subsets, (D) hCD4$^+$:hCD8$^+$ T cell ratios, (E) hTregs, (F) hCD39$^+$ hTregs, (G) hTh17 cells, (H) hTh17:hTreg ratios, (I) hTh1 cells, (J) hTc17 cells, (K) hKIR$^+$hCD8$^+$ cells, (L) hUnconv T cells and (M) hNK cells. Data are presented as the mean ± standard error of the mean (n=3–5). Symbols represent individual mice. Data are from one experiment. Normality was assessed using a Shapiro–Wilk test and significance was tested using (B, C, D, E, F, H, K, L, M) one-way ANOVA or (A, G, I, J) Kruskal–Wallis tests. *P<0.05.

groups compared with the control group. Further, low-dose PTCy increased proportions of hPD-1$^+$hCD4$^+$ and hPD-1$^+$hCD8$^+$ T cells and increased proportions of hPD-1$^+$ hTregs. Finally, this study revealed that high-dose PTCy, but not lower doses, increased proportions of exhausted hCD8$^+$ T cells.

Treatment with low-dose PTCy reduced clinical signs of GVHD, with significantly delayed GVHD onset and increased survival. This was also observed in mice treated with high-dose PTCy, which our group has previously observed [44,47,67]. Markedly, 30% of mice treated with low-dose PTCy survived until the day 70 endpoint. This improved survival with low-dose PTCy also aligns with findings in an allogeneic mouse model [68], where 10 mg/kg PTCy administered on days 3 and 4 was sufficient to reduce GVHD. Conversely, in a recent study in humanised mice, treatment with mid-dose PTCy (25 mg/kg) did not abrogate GVHD development [69], aligning with outcomes in the current study. Therefore, it appears that the efficacy of PTCy is not directly proportional to the dose, with a bimodal response observed. However,

© 2025 The Author(s). This is an open access article published by Portland Press Limited on behalf of the Biochemical Society and distributed under the Creative Commons Attribution License 4.0 (CC BY).

Clinical Science (2025) **139** 1261–1285
https://doi.org/10.1042/CS20257272

given that low-dose PTCy was effective at prolonging survival, this reduced dose may be a better option to reduce toxicity seen with high-dose PTCy treatment.

Treatment with low-dose PTCy increased splenic proportions of hPD-1$^+$hCD4$^+$ and hPD-1$^+$hCD8$^+$ T cells, which were defined as activated T cells [28]. These results align with findings from a recent clinical study, where patients who received PTCy treatment had increased proportions of hPD-1$^+$hCD4$^+$ and hPD-1$^+$hCD8$^+$ T cells from 90 to 180 days post-transplantation [13]. The increased proportions of hPD-1$^+$ T cells observed in humanised mice treated with low-dose PTCy may be related to the pharmacokinetics of cyclophosphamide in mice. A study in BALB/c mice found that a lower dose of 12.5 mg/kg cyclophosphamide led to faster passage of bioactive metabolites from the liver to the bloodstream compared with 25 mg/kg. Additionally, metabolites persisted longer in the bloodstream at a low dose [70]. As such, extended persistence of cyclophosphamide metabolites at a low dose may enhance CD4$^+$ and CD8$^+$ T cell activation, as evidenced by increased proportions of hPD-1$^+$ T cell subsets. It is important to note that enhanced T cell activation does not necessarily equate to enhanced pathogenicity, and these subsets may represent stem-like progenitor exhausted T cells, a precursor to terminally exhausted T cells [71].

Low-dose PTCy, but not higher doses, increased proportions of hPD-1$^+$hCD4$^+$ and hPD-1$^+$hCD8$^+$ T cells, whereas high-dose PTCy, but not lower doses, increased proportions of hPD-1$^+$hLAG3$^+$hCD8$^+$ T cells at the day 70 endpoint. The enrichment of hPD-1$^+$hCD4$^+$ and hPD-1$^+$hCD8$^+$ T cells with low-dose PTCy may reflect an activated or progenitor-exhausted population [72,73], whereas the increase in hPD-1$^+$hLAG3$^+$hCD8$^+$ T cells with high-dose PTCy suggests a shift toward terminal exhaustion [30,74]. However, a limitation of this study is an absence of functional assays for PD-1$^+$ subsets that are required to resolve these states. Future studies utilising proliferation and *ex vivo* restimulation assays with cytokine production analyses would determine whether these cells retain proliferative capacity and effector function or have progressed to terminal exhaustion [74–77]. Additionally, assessment of transcription factors such as TOX (or thymocyte selection-associated high mobility group box protein) and TCF-1 (or T cell factor-1) would distinguish progenitor versus terminal exhaustion states, respectively [78,79]. Nevertheless, activated CD8$^+$ T cells contribute to GVHD pathogenesis in humanised mice [80,81], indicating that the exhausted CD8$^+$ T cell phenotype observed with high-dose PTCy in this study may be contributing to reduced GVHD severity. Further, the increase in hPD-1$^+$hLAG3$^+$hCD8$^+$ T cells does not appear to affect GVL immunity, as this dose of PTCy alone or in combination with other agents does not impair GVL responses in preclinical humanised mouse models [67,82].

PTCy increased hPD-1$^+$hTregs at low, mid and high doses, while low-dose PTCy showed the greatest increase in the proportions of splenic hPD-1$^+$hTregs. Though Tregs can modulate the immune response through the secretion of anti-inflammatory cytokines, Tregs can also inhibit an inflammatory response through cell–cell interactions through PD-1 and LAG3 with their canonical receptor ligands [83,84]. Furthermore, PD-1 signalling plays an important role in maintaining the suppressive capabilities of Tregs [85]. Overall, this suggests that Treg resilience is bolstered by PTCy, which may be a contributing factor to the mechanism by which PTCy reduces GVHD.

Mid-dose PTCy, but not low- or high-dose PTCy, reduced proportions of hLAG3$^+$hCD4$^+$ T cells and hLAG3$^+$ hTregs. A previous study in an allogeneic mouse model, where T cells from LAG3-deficient mice were transplanted into BALB/c mice, found that the absence of LAG3 on CD4$^+$ but not CD8$^+$ T cells exacerbates GVHD [86]. This same study also observed that LAG3-deficient Tregs maintained the ability to suppress the proliferation of alloreactive T cells in a mixed lymphocyte reaction, indicating that LAG3 is not required for Treg function. As such, the reduced proportions of hLAG3$^+$hCD4$^+$ T cells rather than hLAG3$^+$ hTregs could be a contributing factor to the lack of clinical efficacy of PTCy at 25 mg/kg in the current study.

Analysis of other immune cell subsets revealed several differences between mice treated with low-, mid- and high-dose PTCy. Mice treated with high-dose PTCy, but not low or mid doses, showed increased proportions of hTh1 cells and reduced proportions of hTh17 cells in the spleen, with a similar trend observed in the liver at the day 70 endpoint. Given the increase in hTh1 cells, which are widely considered the principal CD4$^+$ T cell mediators of GVHD [54,87], these cells could be a contributing factor as to why mice treated with high-dose PTCy still succumb to the disease. Although the role of Th17 cells in GVHD is complex, this subset likely contributes to GVHD pathogenesis [88–90]. As such, the reduced proportions of hTh17 cells observed in high-dose PTCy-treated mice may contribute to the reduced GVHD severity observed in these mice. As this trend was not observed in mice treated with low-dose PTCy,

© 2025 The Author(s). This is an open access article published by Portland Press Limited on behalf of the Biochemical Society and distributed under the Creative Commons Attribution License 4.0 (CC BY).

these outcomes provide further evidence to suggest that PTCy may be reducing GVHD through different dose-dependent mechanisms.

Several studies have observed a role for NK cells in the pathogenesis of GVHD [91,92]. However, NK cells may also protect against GVHD. Several studies demonstrate that grafts containing higher numbers of NK cells and higher NK cell alloreactivity are associated with less severe GVHD [93–95]. In the current study, proportions of splenic and hepatic hNK cells were not reduced in mice treated with low-dose PTCy but were significantly reduced at day 28 in mice treated with mid-dose PTCy. The recovery of NK cells following alloHSCT has been identified as a risk marker for overall survival, with rates of relapse and non-relapse mortality significantly higher in patients with low NK cell counts of <50.5 cells/μl on day 28 post-transplant [96]. As such, the reduced proportions of hNK cells in mice treated with mid-dose PTCy early in disease may be a contributing factor as to why this treatment did not improve clinical GVHD outcomes in the current study.

Despite the delayed disease onset and prolonged survival of mice treated with low- or high-dose PTCy, there were no significant differences in histological GVHD in any of the target organs examined at day 70. The absence of histological improvements may be due to most mice having reached advanced disease by endpoint, potentially obscuring earlier treatment effects. However, there was a downward trend in liver GVHD at day 28 in mice treated with low- or high-dose PTCy. This trend is consistent with reduced liver GVHD in humanised mice treated with 33 mg/kg PTCy [44,47] and in allogeneic mice treated with 10 mg/kg PTCy [20]. Reasons for the differing magnitude of liver GVHD in humanised mice treated with high-dose PTCy remain unknown but may reflect donor differences or the heterogeneity of organ involvement in GVHD development.

A limitation of this study is that PTCy dosing in mice cannot be directly equated to clinical regimens due to species differences in body surface area, metabolism and pharmacokinetics. Given that NSG mice are more sensitive than humans to chemotherapy [97], 33 mg/kg PTCy represents an appropriate high dose in this model and was selected based on allogeneic mouse models of GVHD [24]. Our group has previously shown that this dose effectively reduces alloreactive donor T cell proliferation and GVHD [44] without compromising GVL immunity [82], supporting its value as a clinically relevant framework for dissecting the cellular mechanisms underlying PTCy efficacy in GVHD. Moreover, findings from the short-term model are constrained by the small sample size, and confirmation of these outcomes in larger cohorts is warranted.

The clinical implications of dose modification are considerable, given the well-established toxicities of cyclophosphamide at higher doses [98]. However, our study did not include direct measures of PTCy-associated toxicity. Future studies should incorporate toxicity assessments alongside efficacy, including (i) echocardiography with cardiac TUNEL (or terminal deoxynucleotidyl transferase dUTP nick end labeling) staining for cardiotoxicity [99,100]; (ii) daily urinalysis with bladder histology for urothelial injury [101]; (iii) liver function measurements of alanine aminotransferase, aspartate aminotransferase, alkaline phosphatase and total bilirubin for hepatotoxicity [102,103]; and (iv) renal function measurements of blood urea nitrogen and creatinine for nephrotoxicity [104]. To disentangle toxicity from GVHD-associated injury, these readouts should be evaluated in GVHD and non-GVHD cohorts receiving identical PTCy treatment regimens.

To conclude, this study aimed to determine the efficacy of lower doses of PTCy for GVHD attenuation and the subsequent effects on tissue damage and immune cell subsets at early and late time points in GVHD development using a preclinical humanised mouse model. Together, results from this study indicate that low-dose PTCy (10 mg/kg) reduces GVHD at a similar efficacy to high-dose PTCy (33 mg/kg). Moreover, the reduction in GVHD appears to be occurring through different dose-dependent mechanisms. Low-dose PTCy spared $hCD8^+$ T cell exhaustion and increased proportions of $hPD\text{-}1^+hCD4^+$ T cells, $hPD\text{-}1^+hCD8^+$ T cells and $PD\text{-}1^+$ hTregs. Conversely, high-dose PTCy led to a trending increase in hTh1 cell proportions and increased proportions of exhausted $hCD8^+$ T cells. While an increase in exhausted $hCD8^+$ T cells following treatment with high-dose PTCy may be beneficial for GVHD prevention, this may pose deleterious effects on GVL immunity. Therefore, treatment with low-dose PTCy, which increases T cell activation and avoids $hCD8^+$ T cell exhaustion, may enhance GVL immunity, but further investigation into this notion is required. Furthermore, while low-dose PTCy attenuates GVHD, mice still succumb to disease. As such, future studies should investigate additional therapeutics to combine with low-dose PTCy to further improve clinical outcomes.

© 2025 The Author(s). This is an open access article published by Portland Press Limited on behalf of the Biochemical Society and distributed under the Creative Commons Attribution License 4.0 (CC BY).

Clinical Science (2025) **139** 1261–1285
https://doi.org/10.1042/CS20257272

Clinical Perspectives

- Post-transplant cyclophosphamide (PTCy) is used to prevent graft-versus-host disease (GVHD) following allogeneic haematopoietic stem cell transplantation (alloHSCT), but GVHD still develops in 40-50% of patients, necessitating a deeper understanding of its cellular mechanisms of action.
- Findings from this study demonstrate that low-dose PTCy can reduce GVHD with similar efficacy as high-dose PTCy in a preclinical humanised mouse model, with disease attenuation associated with different dose-dependent cellular mechanisms.
- These findings suggest that a lower PTCy dose may improve outcomes for alloHSCT recipients.

Data Availability

The data that support the findings of this study are available from the corresponding author upon reasonable request.

Competing Interests

The authors declare that there are no competing interests associated with the manuscript.

Funding

The authors acknowledge funding from the Australian Government Research Training Program (to CS and AE), University of Wollongong RevITAlise (RITA) Research Grant Scheme (grant number T021; to RS and DW), donations from John and Betsie van Schelven (to RS) and an Australian and New Zealand Society for Immunology (ASI) Breakthrough Immunology Award (to DW).

Open Access

This article has been published open access under our Subscribe to Open programme, made possible through the support of our subscribing institutions, learn more here: https://portlandpress.com/pages/open_access_options_and_prices#conditional

CRediT Author Contribution

C.S. contributed to Writing – Original Draft, Conceptualisation, Supervision, Writing – Review & Editing, Data Curation, Investigation, Formal Analysis, Methodology and Visualisation. M.J.J. contributed to Writing – Review & Editing and Investigation. A.E. contributed to Writing – Review & Editing and Investigation. R.S. contributed to Conceptualisation, Funding Acquisition, Project Administration, Supervision, Writing – Review & Editing, Data Curation, Resources, Formal Analysis and Methodology. D.W. contributed to Conceptualisation, Funding Acquisition, Project Administration, Supervision, Writing – Review & Editing, Data Curation, Resources, Formal Analysis and Methodology.

Acknowledgments

The authors acknowledge the University of Wollongong and Molecular Horizons technical staff, the Molecular Horizons Fluorescence Analysis Facility and Molecular Horizons Animal Research Facility technical staff.

Abbreviations

ANOVA, analysis of variance; Ctrl, control; FSC-A, forward scatter area; FSC-H, forward scatter height; GVHD, graft-versus-host disease; GVL, graft-versus-leukaemia; IL, interleukin; KIR, killer cell immunoglobulin-like receptor; MST, median survival time; NIR, near infrared; NK, natural killer; NSG, NOD-scid-IL2Rγ^{null}; PBS, phosphate buffered saline; PTCy, post-transplant cyclophosphamide; SSC-A, side scatter area; Tc, cytotoxic T; Tcon, conventional T; Th, T helper; Treg, regulatory T cell; Unconv, unconventional; alloHSCT, allogeneic

© 2025 The Author(s). This is an open access article published by Portland Press Limited on behalf of the Biochemical Society and distributed under the Creative Commons Attribution License 4.0 (CC BY).

haematopoietic stem cell transplantation; alloHSCT, allogeneic haematopoietic stem cell transplantation; h, human; hPBMC, human peripheral blood mononuclear cell; i.p., intraperitoneally.

References

1 Copelan, E.A. (2006) Hematopoietic stem-cell transplantation. *N. Engl. J. Med.* **354**, 1813–1826 https://doi.org/10.1056/NEJMra052638 PMID: 16641398
2 Dickinson, A.M., Norden, J., Li, S., Hromadnikova, I., Schmid, C., Schmetzer, H. et al. (2017) Graft-versus-leukemia effect following hematopoietic stem cell transplantation for leukemia. *Front. Immunol.* **8**, 496, 496 https://doi.org/10.3389/fimmu.2017.00496 PMID: 28638379
3 Glucksberg, H., Storb, R., Fefer, A., Buckner, C.D., Neiman, P.E., Clift, R.A. et al. (1974) Clinical manifestations of graft-versus-host disease in human recipients of marrow from HL-A-matched sibling donors. *Transplantation* **18**, 295–304 https://doi.org/10.1097/00007890-197410000-00001 PMID: 4153799
4 Jagasia, M., Arora, M., Flowers, M.E.D., Chao, N.J., McCarthy, P.L., Cutler, C.S, et al. (2012) Risk factors for acute GVHD and survival after hematopoietic cell transplantation. *Blood* **119**, 296–307 https://doi.org/10.1182/blood-2011-06-364265 PMID: 22010102
5 Khurshid, I. and Anderson, L.C. (2002) Non-infectious pulmonary complications after bone marrow transplantation. *Postgrad. Med. J.* **78**, 257–262 https://doi.org/10.1136/pmj.78.919.257 PMID: 12151565
6 Kanakry, C.G., Ganguly, S., Zahurak, M., Bolaños-Meade, J., Thoburn, C., Perkins, B. et al. (2013) Aldehyde dehydrogenase expression drives human regulatory T cell resistance to posttransplantation cyclophosphamide. *Sci. Transl. Med.* **5**, 211ra157 https://doi.org/10.1126/scitranslmed.3006960 PMID: 24225944
7 Kanakry, C.G., O'Donnell, P.V., Furlong, T., De Lima, M.J., Wei, W., Medeot, M, et al. (2014) Multi-institutional study of post-transplantation cyclophosphamide as single-agent graft-versus-host disease prophylaxis after allogeneic bone marrow transplantation using myeloablative busulfan and fludarabine conditioning. *J. Clin. Oncol* **32**, 3497–3505 https://doi.org/10.1200/JCO.2013.54.0625 PMID: 25267759
8 Luznik, L., Bolaños-Meade, J., Zahurak, M., Chen, A.R., Smith, B.D., Brodsky, R, et al. (2010) High-dose cyclophosphamide as single-agent, short-course prophylaxis of graft-versus-host disease. *Blood* **115**, 3224–3230 https://doi.org/10.1182/blood-2009-11-251595 PMID: 20124511
9 Luznik, L. and Fuchs, E.J. (2010) High-dose, post-transplantation cyclophosphamide to promote graft-host tolerance after allogeneic hematopoietic stem cell transplantation. *Immunol. Res.* **47**, 65–77 https://doi.org/10.1007/s12026-009-8139-0 PMID: 20066512
10 Munchel, A., Kesserwan, C., Symons, H.J., Luznik, L., Kasamon, Y.L., Jones, R.J. et al. (2011) Nonmyeloablative, HLA-haploidentical bone marrow transplantation with high dose, post-transplantation cyclophosphamide. *Pediatr. Rep.* **3 Suppl 2**, e15 https://doi.org/10.4081/pr.2011.s2.e15 PMID: 22053277
11 Khimani, F., Ranspach, P., Elmariah, H., Kim, J., Whiting, J., Nishihori, T, et al. (2021) Increased infections and delayed $CD4^+$ T cell but faster B cell immune reconstitution after post-transplantation cyclophosphamide compared to conventional GVHD prophylaxis in allogeneic transplantation. *Transplant. Cell. Ther* **27**, 940–948 https://doi.org/10.1016/j.jtct.2021.07.023 PMID: 34329754
12 Stocker, N., Gaugler, B., Labopin, M., Farge, A., Ye, Y., Ricard, L. et al. (2020) High-dose post-transplant cyclophosphamide impairs γδ T-cell reconstitution after haploidentical haematopoietic stem cell transplantation using low-dose antithymocyte globulin and peripheral blood stem cell graft. *Clin. Transl. Immunology* **9**, e1171 https://doi.org/10.1002/cti2.1171 PMID: 33005413
13 Zhao, C., Bartock, M., Jia, B., Shah, N., Claxton, D.F., Wirk, B, et al. (2022) Post-transplant cyclophosphamide alters immune signatures and leads to impaired T cell reconstitution in allogeneic hematopoietic stem cell transplant. *J. Hematol. Oncol* **15**, 64 https://doi.org/10.1186/s13045-022-01287-3 PMID: 35590334
14 Emadi, A., Jones, R.J. and Brodsky, R.A. (2009) Cyclophosphamide and cancer: golden anniversary. *Nat. Rev. Clin. Oncol* **6**, 638–647 https://doi.org/10.1038/nrclinonc.2009.146 PMID: 19786984
15 Duléry, R., Mohty, R., Labopin, M., Sestili, S., Malard, F., Brissot, E. et al. (2021) Early cardiac toxicity associated with post-transplant cyclophosphamide in allogeneic stem cell transplantation. *JACC CardioOncol.* **3**, 250–259 https://doi.org/10.1016/j.jaccao.2021.02.011 PMID: 34396331
16 McDonald, G.B., Slattery, J.T., Bouvier, M.E., Ren, S., Batchelder, A.L., Kalhorn, T.F. et al. (2003) Cyclophosphamide metabolism, liver toxicity, and mortality following hematopoietic stem cell transplantation. *Blood* **101**, 2043–2048 https://doi.org/10.1182/blood-2002-06-1860 PMID: 12406916
17 Travis, L.B., Curtis, R.E., Glimelius, B., Holowaty, E.J., Van Leeuwen, F.E., Lynch, C.F, et al. (1995) Bladder and kidney cancer following cyclophosphamide therapy for non-Hodgkin's lymphoma. *JNCI Journal of the National Cancer Institute* **87**, 524–531 https://doi.org/10.1093/jnci/87.7.524 PMID: 7707439
18 Koklu, H., Tufan, A., Erkul, Y., Akyurek, N. and Civelek, R. (2015) Secondary acute myeloid leukemia arising early after cyclophosphamide treatment. *Int. J. Clin. Pharm.* **37**, 289–291 https://doi.org/10.1007/s11096-015-0069-4 PMID: 25612567
19 Wachsmuth, L.P., Patterson, M.T., Eckhaus, M.A., Venzon, D.J., Gress, R.E. and Kanakry, C.G. (2019) Post-transplantation cyclophosphamide prevents graft-versus-host disease by inducing alloreactive T cell dysfunction and suppression. *J. Clin. Invest.* **129**, 2357–2373, 124218 https://doi.org/10.1172/JCI124218 PMID: 30913039
20 Wang, Y., Chang, Y.-J., Chen, L., Xu, L.-P., Bian, Z.-L., Zhang, X.-H. et al. (2017) Low-dose post-transplant cyclophosphamide can mitigate GVHD and enhance the G-CSF/ATG induced GVHD protective activity and improve haploidentical transplant outcomes. *Oncoimmunology* **6**, e1356152 https://doi.org/10.1080/2162402X.2017.1356152 PMID: 29147612
21 Wang, Y., Wu, D.-P., Liu, Q.F., Xu, L.P., Liu, K.Y., Zhang, X.H. et al. (2019) Low-dose post-transplant cyclophosphamide and anti-thymocyte globulin as an effective strategy for GVHD prevention in haploidentical patients. *J. Hematol. Oncol.* **12**, 88 https://doi.org/10.1186/s13045-019-0781-y PMID: 31481121
22 Duléry, R., Goudet, C., Mannina, D., Bianchessi, A., Granata, A., Harbi, S. et al. (2023) Reduced post-transplant cyclophosphamide doses in haploidentical hematopoietic cell transplantation for elderly patients with hematological malignancies. *Bone Marrow Transplant.* **58**, 386–392 https://doi.org/10.1038/s41409-022-01908-y PMID: 36585459

© 2025 The Author(s). This is an open access article published by Portland Press Limited on behalf of the Biochemical Society and distributed under the Creative Commons Attribution License 4.0 (CC BY).

23 Eto, M., Mayumi, H., Tomita, Y., Yoshikai, Y., Nishimura, Y. and Nomoto, K. (1990) Sequential mechanisms of cyclophosphamide-induced skin allograft tolerance including the intrathymic clonal deletion followed by late breakdown of the clonal deletion. *J. Immunol.* **145**, 1303–1310 https://doi.org/10.4049/jimmunol.145.5.1303 PMID: 2143514
24 Ganguly, S., Ross, D.B., Panoskaltsis-Mortari, A., Kanakry, C.G., Blazar, B.R., Levy, R.B. et al. (2014) Donor $CD4^+$ $Foxp3^+$ regulatory T cells are necessary for posttransplantation cyclophosphamide-mediated protection against GVHD in mice. *Blood* **124**, 2131–2141 https://doi.org/10.1182/blood-2013-10-525873 PMID: 25139358
25 Wherry, E.J. (2011) T cell exhaustion. *Nat. Immunol.* **12**, 492–499 https://doi.org/10.1038/ni.2035 PMID: 21739672
26 Wherry, E.J. and Kurachi, M. (2015) Molecular and cellular insights into T cell exhaustion. *Nat. Rev. Immunol.* **15**, 486–499 https://doi.org/10.1038/nri3862 PMID: 26205583
27 Gianchecchi, E. and Fierabracci, A. (2018) Inhibitory receptors and pathways of lymphocytes: the role of PD-1 in Treg development and their involvement in autoimmunity onset and cancer progression. *Front. Immunol.* **9**, 2374, 2374 https://doi.org/10.3389/fimmu.2018.02374 PMID: 30386337
28 Aksoylar, H.I. and Boussiotis, V.A. (2020) PD-1^+ Treg cells: A foe in cancer immunotherapy? *Nat. Immunol* **21**, 1311–1312 https://doi.org/10.1038/s41590-020-0801-7 PMID: 32973361
29 Goldberg, M.V. and Drake, C.G. (2011) LAG-3 in cancer immunotherapy. *Curr. Top. Microbiol. Immunol.* **344**, 269–278 https://doi.org/10.1007/82_2010_114 PMID: 21086108
30 Pauken, K.E. and Wherry, E.J. (2015) Snapshot: T cell exhaustion. *Cell* **163**, 1038–1038 https://doi.org/10.1016/j.cell.2015.10.054 PMID: 26544946
31 Zhou, M., Sacirbegovic, F., Zhao, K., Rosenberger, S. and Shlomchik, W.D. (2020) T cell exhaustion and a failure in antigen presentation drive resistance to the graft-versus-leukemia effect. *Nat. Commun.* **11**, 4227, 4227 https://doi.org/10.1038/s41467-020-17991-y PMID: 32839441
32 Liu, L., Chang, Y.J., Xu, L.P., Zhang, X.H., Wang, Y., Liu, K.Y, et al. (2018) Reversal of T cell exhaustion by the first donor lymphocyte infusion is associated with the persistently effective antileukemic responses in patients with relapsed AML after allo-HSCT. *Biol. Blood Marrow Transplant* **24**, 1350–1359 https://doi.org/10.1016/j.bbmt.2018.03.030 PMID: 29649617
33 Liu, L., Chang, Y.-J., Xu, L.-P., Zhang, X.-H., Wang, Y., Liu, K.-Y, et al. (2018) T cell exhaustion characterized by compromised MHC class I and II restricted cytotoxic activity associates with acute B lymphoblastic leukemia relapse after allogeneic hematopoietic stem cell transplantation. *Clin. Immunol.* **190**, 32–40 https://doi.org/10.1016/j.clim.2018.02.009 PMID: 29477343
34 Matthews, K., Lim, Z., Afzali, B., Pearce, L., Abdallah, A., Kordasti, S. et al. (2009) Imbalance of effector and regulatory CD4 T cells is associated with graft-versus-host disease after hematopoietic stem cell transplantation using a reduced intensity conditioning regimen and alemtuzumab. *Haematologica* **94**, 956–966 https://doi.org/10.3324/haematol.2008.003103 PMID: 19491336
35 Taylor, P.A., Lees, C.J. and Blazar, B.R. (2002) The infusion of *ex vivo* activated and expanded $CD4^+CD25^+$ immune regulatory cells inhibits graft-versus-host disease lethality. *Blood* **99**, 3493–3499 https://doi.org/10.1182/blood.V99.10.3493 PMID: 11986199
36 Collison, L.W., Workman, C.J., Kuo, T.T., Boyd, K., Wang, Y., Vignali, K.M. et al. (2007) The inhibitory cytokine IL-35 contributes to regulatory T-cell function. *Nature* **450**, 566–569 https://doi.org/10.1038/nature06306 PMID: 18033300
37 Sage, P.T., Francisco, L.M., Carman, C.V. and Sharpe, A.H. (2013) The receptor PD-1 controls follicular regulatory T cells in the lymph nodes and blood. *Nat. Immunol.* **14**, 152–161 https://doi.org/10.1038/ni.2496 PMID: 23242415
38 Ikegawa, S., Meguri, Y., Kondo, T., Sugiura, H., Sando, Y., Nakamura, M. et al. (2019) PTCy ameliorates GVHD by restoring regulatory and effector T-cell homeostasis in recipients with PD-1 blockade. *Blood Adv.* **3**, 4081–4094 https://doi.org/10.1182/bloodadvances.2019000134 PMID: 31821459
39 Lidster, K., Owen, K., Browne, W.J. and Prescott, M.J. (2019) Cage aggression in group-housed laboratory male mice: An international data crowdsourcing project. *Sci. Rep.* **9**, 15211, 15211 https://doi.org/10.1038/s41598-019-51674-z PMID: 31645617
40 Adhikary, S.R., Geraghty, N.J., Cuthbertson, P., Sluyter, R. and Watson, D. (2019) Altered donor P2X7 activity in human leukocytes correlates with P2RX7 genotype but does not affect the development of graft-versus-host disease in humanised mice. *Purinergic Signal.* **15**, 177–192 https://doi.org/10.1007/s11302-019-09651-8 PMID: 31001750
41 Hu, M., Hawthorne, W.J., Nicholson, L., Burns, H., Qian, Y.W., Liuwantara, D, et al. (2020) Low-dose interleukin-2 combined with rapamycin led to an expansion of $CD4^+CD25^+FOXP3^+$ regulatory T cells and prolonged human islet allograft survival in humanized mice. *Diabetes* **69**, 1735–1748 https://doi.org/10.2337/db19-0525 PMID: 32381646
42 Schindelin, J., Arganda-Carreras, I., Frise, E., Kaynig, V., Longair, M., Pietzsch, T. et al. (2012) Fiji: an open-source platform for biological-image analysis. *Nat. Methods* **9**, 676–682 https://doi.org/10.1038/nmeth.2019 PMID: 22743772
43 Cuthbertson, P., Adhikary, S.R., Geraghty, N.J., Guy, T.V., Hadjiashrafi, A., Fuller, S.J, et al. (2020) Increased P2X7 expression in the gastrointestinal tract and skin in a humanised mouse model of graft-versus-host disease. *Clin. Sci* **134**, 207–223 https://doi.org/10.1042/CS20191086 PMID: 31934722
44 Adhikary, S.R., Cuthbertson, P., Nicholson, L., Bird, K.M., Sligar, C., Hu, M. et al. (2021) Post-transplant cyclophosphamide limits reactive donor T cells and delays the development of graft-versus-host disease in a humanized mouse model. *Immunology* **164**, 332–347 https://doi.org/10.1111/imm.13374 PMID: 34021907
45 Ledingham, D., Plant, M., Mustafa, F. and Patil, B. (2020) Preserving fertility: using cyclophosphamide and other cytotoxics in young people. *Pract Neurol (Fort Wash Pa)* **20**, 148–153 https://doi.org/10.1136/practneurol-2019-002247 PMID: 31519764
46 Geraghty, N.J., Belfiore, L., Adhikary, S.R., Alexander, S.I., Sluyter, R. and Watson, D. (2019) Increased splenic human $CD4^+$:$CD8^+$ T cell ratios, serum human interferon-γ and intestinal human interleukin-17 are associated with clinical graft-versus-host disease in humanized mice. *Transpl. Immunol* **54**, 38–46 https://doi.org/10.1016/j.trim.2019.02.003 PMID: 30743002
47 Sligar, C., Cuthbertson, P., Miles, N.A., Adhikary, S.R., Elhage, A., Zhang, G. et al. (2023) Tocilizumab increases regulatory T cells, reduces natural killer cells and delays graft-versus-host disease development in humanized mice treated with post-transplant cyclophosphamide. *Immunol. Cell Biol.* **101**, 639–656 https://doi.org/10.1111/imcb.12652 PMID: 37191045
48 Huttunen, P., Taskinen, M., Siitonen, S. and Saarinen-Pihkala, U.M. (2015) Impact of very early CD4(+) /CD8(+) T cell counts on the occurrence of acute graft-versus-host disease and NK cell counts on outcome after pediatric allogeneic hematopoietic stem cell transplantation. *Pediatr. Blood Cancer* **62**, 522–528 https://doi.org/10.1002/pbc.25347 PMID: 25417898

© 2025 The Author(s). This is an open access article published by Portland Press Limited on behalf of the Biochemical Society and distributed under the Creative Commons Attribution License 4.0 (CC BY).

49 Budde, H., Papert, S., Maas, J.H., Reichardt, H.M., Wulf, G., Hasenkamp, J. et al. (2017) Prediction of graft-versus-host disease: a biomarker panel based on lymphocytes and cytokines. *Ann. Hematol.* **96**, 1127–1133 https://doi.org/10.1007/s00277-017-2999-5 PMID: 28447161
50 Sakaguchi, S., Sakaguchi, N., Asano, M., Itoh, M. and Toda, M. (1995) Immunologic self-tolerance maintained by activated T cells expressing IL-2 receptor alpha-chains (CD25). Breakdown of a single mechanism of self-tolerance causes various autoimmune diseases. *J. Immunol.* **155**, 1151–1164 https://doi.org/10.4049/jimmunol.155.3.1151 PMID: 7636184
51 Gu, J., Ni, X., Pan, X., Lu, H., Lu, Y., Zhao, J. et al. (2017) Human CD39^{hi} regulatory T cells present stronger stability and function under inflammatory conditions. *Cell. Mol. Immunol.* **14**, 521–528 https://doi.org/10.1038/cmi.2016.30 PMID: 27374793
52 Gartlan, K.H., Varelias, A., Koyama, M., Robb, R.J., Markey, K.A., Chang, K. et al. (2017) Th17 plasticity and transition toward a pathogenic cytokine signature are regulated by cyclosporine after allogeneic SCT. *Blood Adv.* **1**, 341–351 https://doi.org/10.1182/bloodadvances.2016002980 PMID: 29296949
53 Hill, G.R., Crawford, J.M., Cooke, K.R., Brinson, Y.S., Pan, L. and Ferrara, J.L. (1997) Total body irradiation and acute graft-versus-host disease: the role of gastrointestinal damage and inflammatory cytokines. *Blood* **90**, 3204–3213 PMID: 9376604,
54 Fu, J., Wu, Y., Nguyen, H., Heinrichs, J., Schutt, S., Liu, Y. et al. (2016) T-bet promotes acute graft-versus-host disease by regulating recipient hematopoietic cells in mice. *J. Immunol.* **196**, 3168–3179 https://doi.org/10.4049/jimmunol.1501020 PMID: 26903480
55 Gartlan, K.H., Markey, K.A., Varelias, A., Bunting, M.D., Koyama, M., Kuns, R.D. et al. (2015) Tc17 cells are a proinflammatory, plastic lineage of pathogenic CD8$^+$ T cells that induce GVHD without antileukemic effects. *Blood* **126**, 1609–1620 https://doi.org/10.1182/blood-2015-01-622662 PMID: 26206951
56 Li, J., Zaslavsky, M., Su, Y., Guo, J., Sikora, M.J., Unen, V, et al. (2022) KIR$^+$CD8$^+$ T cells suppress pathogenic T cells and are active in autoimmune diseases and COVID-19. *Science* **376**, eabi9591 https://doi.org/10.1126/science.abi9591 PMID: 35258337
57 Chen, X., Ghanizada, M., Mallajosyula, V., Sola, E., Capasso, R., Kathuria, K.R, et al. (2025) Differential roles of human CD4$^+$ and CD8$^+$ regulatory T cells in controlling self-reactive immune responses. *Nat. Immunol* **26**, 230–239 https://doi.org/10.1038/s41590-024-02062-x PMID: 39806065
58 Godfrey, D.I., Uldrich, A.P., McCluskey, J., Rossjohn, J. and Moody, D.B. (2015) The burgeoning family of unconventional T cells. *Nat. Immunol.* **16**, 1114–1123 https://doi.org/10.1038/ni.3298 PMID: 26482978
59 Wu, N., Liu, R., Liang, S., Gao, H., Xu, L.-P., Zhang, X.-H. et al. (2021) γδ T cells may aggravate acute graft-versus-host disease through CXCR4 signaling after allogeneic hematopoietic transplantation. *Front. Immunol.* **12**, 687961 https://doi.org/10.3389/fimmu.2021.687961 PMID: 34335589
60 Zeng, D., Lewis, D., Dejbakhsh-Jones, S., Lan, F., García-Ojeda, M., Sibley, R. et al. (1999) Bone marrow NK1.1(-) and NK1.1(+) T cells reciprocally regulate acute graft versus host disease. *J. Exp. Med.* **189**, 1073–1081 https://doi.org/10.1084/jem.189.7.1073 PMID: 10190898
61 Lan, F., Zeng, D., Higuchi, M., Huie, P., Higgins, J.P. and Strober, S. (2001) Predominance of NK1.1$^+$TCR alpha beta$^+$ or DX5$^+$TCR alpha beta$^+$ T cells in mice conditioned with fractionated lymphoid irradiation protects against graft-versus-host disease: "natural suppressor" cells. *J. Immunol.* **167**, 2087–2096 https://doi.org/10.4049/jimmunol.167.4.2087 PMID: 11489992
62 Cuthbertson, P., Geraghty, N.J., Adhikary, S.R., Casolin, S., Watson, D. and Sluyter, R. (2021) P2X7 receptor antagonism increases regulatory T cells and reduces clinical and histological graft-versus-host disease in a humanised mouse model. *Clin. Sci* **135**, 495–513 https://doi.org/10.1042/CS20201352 PMID: 33463682
63 Olson, J.A., Leveson-Gower, D.B., Gill, S., Baker, J., Beilhack, A. and Negrin, R.S. (2010) NK cells mediate reduction of GVHD by inhibiting activated, alloreactive T cells while retaining GVT effects. *Blood* **115**, 4293–4301 https://doi.org/10.1182/blood-2009-05-222190 PMID: 20233969
64 Malard, F., Holler, E., Sandmaier, B.M., Huang, H. and Mohty, M. (2023) Acute graft-versus-host disease. *Nat. Rev. Dis. Primers* **9**, 27 https://doi.org/10.1038/s41572-023-00438-1 PMID: 37291149
65 Fujii, H., Luo, Z.-J., Kim, H.J., Newbigging, S., Gassas, A., Keating, A. et al. (2015) Humanized chronic graft-versus-host disease in NOD-SCID il2rγ-/- (NSG) mice with G-CSF-mobilized peripheral blood mononuclear cells following cyclophosphamide and total body irradiation. *PLOS ONE* **10**, e0133216 https://doi.org/10.1371/journal.pone.0133216 PMID: 26176698
66 Nunes, N.S. and Kanakry, C.G. (2019) Mechanisms of graft-versus-host disease prevention by post-transplantation cyclophosphamide: an evolving understanding. *Front. Immunol.* **10**, 2668, 2668 https://doi.org/10.3389/fimmu.2019.02668 PMID: 31849930
67 Cuthbertson, P., Button, A., Sligar, C., Elhage, A., Vine, K.L., Watson, D. et al. (2024) Post-transplant cyclophosphamide combined with Brilliant Blue G reduces graft-versus-host disease without compromising graft-versus-leukaemia immunity in humanised mice. *Int. J. Mol. Sci.* **25**, 1775 https://doi.org/10.3390/ijms25031775 PMID: 38339054
68 Wachsmuth, L.P., Patterson, M.T., Eckhaus, M.A., Venzon, D.J. and Kanakry, C.G. (2020) Optimized timing of post-transplantation cyclophosphamide in MHC-haploidentical murine hematopoietic cell transplantation. *Biol. Blood Marrow Transplant.* **26**, 230–241 https://doi.org/10.1016/j.bbmt.2019.09.030 PMID: 31586477
69 Gilman, K.E., Cracchiolo, M.J., Matiatos, A.P., Davini, D.W., Simpson, R.J. and Katsanis, E. (2022) Partially replacing cyclophosphamide with bendamustine in combination with cyclosporine A improves survival and reduces xenogeneic graft-versus-host-disease. *Front. Immunol.* **13**, 1045710 https://doi.org/10.3389/fimmu.2022.1045710 PMID: 36700195
70 Pukhalsky, A.L., Toptygina, A.P. and Viktorov, V.V. (1990) Pharmacokinetics of alkylating metabolites of cyclophosphamide in different strains of mice. *Int. J. Immunopharmacol.* **12**, 217–223 https://doi.org/10.1016/0192-0561(90)90056-s PMID: 2329014
71 Waibl Polania, J., Hoyt-Miggelbrink, A., Tomaszewski, W.H., Wachsmuth, L.P., Lorrey, S.J., Wilkinson, D.S, et al. (2025) Antigen presentation by tumor-associated macrophages drives T cells from a progenitor exhaustion state to terminal exhaustion. *Immunity* **58**, 232–246 https://doi.org/10.1016/j.immuni.2024.11.026 PMID: 39724910
72 Siddiqui, I., Schaeuble, K., Chennupati, V., Fuertes Marraco, S.A., Calderon-Copete, S., Pais Ferreira, D, et al. (2019) Intratumoral Tcf1$^+$PD-1$^+$CD8$^+$ T cells with stem-like properties promote tumor control in response to vaccination and checkpoint blockade immunotherapy. *Immunity* **50**, 195–211 https://doi.org/10.1016/j.immuni.2018.12.021 PMID: 30635237
73 Ahn, E., Araki, K., Hashimoto, M., Li, W., Riley, J.L., Cheung, J. et al. (2018) Role of PD-1 during effector CD8 T cell differentiation. *Proc. Natl. Acad. Sci. U.S.A.* **115**, 4749–4754 https://doi.org/10.1073/pnas.1718217115 PMID: 29654146

© 2025 The Author(s). This is an open access article published by Portland Press Limited on behalf of the Biochemical Society and distributed under the Creative Commons Attribution License 4.0 (CC BY).

74 Hofmann, M., Thimme, R. and Schamel, W.W. (2024) PD-1 and LAG-3: synergistic fostering of T cell exhaustion. *Signal Transduct. Target. Ther.* **9**, 291, 291 https://doi.org/10.1038/s41392-024-02000-1 PMID: 39424778

75 Petrelli, A., Mijnheer, G., Hoytema van Konijnenburg, D.P., Van der Wal, M.M., Giovannone, B., Mocholi, E, et al. (2018) PD-1^{+}CD8^{+} T cells are clonally expanding effectors in human chronic inflammation. *J. Clin. Invest* **128**, 4669–4681, 96107 https://doi.org/10.1172/JCI96107 PMID: 30198907

76 Balança, C.-C., Salvioni, A., Scarlata, C.-M., Michelas, M., Martinez-Gomez, C., Gomez-Roca, C. et al. (2021) PD-1 blockade restores helper activity of tumor-infiltrating, exhausted PD-1^{hi}CD39^{+} CD4 T cells. *JCI Insight* **6**, e142513 https://doi.org/10.1172/jci.insight.142513 PMID: 33332284

77 Im, S.J., Hashimoto, M., Gerner, M.Y., Lee, J., Kissick, H.T., Burger, M.C. et al. (2016) Defining CD8^{+} T cells that provide the proliferative burst after PD-1 therapy. *Nature* **537**, 417–421 https://doi.org/10.1038/nature19330 PMID: 27501248

78 Khan, O., Giles, J.R., McDonald, S., Manne, S., Ngiow, S.F., Patel, K.P. et al. (2019) TOX transcriptionally and epigenetically programs CD8^{+} T cell exhaustion. *Nature* **571**, 211–218 https://doi.org/10.1038/s41586-019-1325-x PMID: 31207603

79 Utzschneider, D.T., Charmoy, M., Chennupati, V., Pousse, L., Ferreira, D.P., Calderon-Copete, S, et al. (2016) T cell factor 1-expressing memory-like CD8^{+} T cells sustain the immune response to chronic viral infections. *Immunity* **45**, 415–427 https://doi.org/10.1016/j.immuni.2016.07.021 PMID: 27533016

80 King, M., Pearson, T., Rossini, A.A., Shultz, L.D. and Greiner, D.L. (2008) Humanized mice for the study of type 1 diabetes and beta cell function. *Ann. N. Y. Acad. Sci.* **1150**, 46–53 https://doi.org/10.1196/annals.1447.009 PMID: 19120266

81 Kawasaki, Y., Sato, K., Hayakawa, H., Takayama, N., Nakano, H., Ito, R, et al. (2018) Comprehensive analysis of the activation and proliferation kinetics and effector functions of human lymphocytes, and antigen presentation capacity of antigen-presenting cells in xenogeneic graft-versus-host disease. *Biol. Blood Marrow Transplant* **24**, 1563–1574 https://doi.org/10.1016/j.bbmt.2018.04.016 PMID: 29678638

82 Sligar, C., Reilly, E., Cuthbertson, P., Vine, K.L., Bird, K.M., Elhage, A. et al. (2024) Graft-versus-leukaemia immunity is retained following treatment with post-transplant cyclophosphamide alone or combined with tocilizumab in humanised mice. *Clin. Transl. Immunology* **13**, e1497, e1497 https://doi.org/10.1002/cti2.1497 PMID: 38495918

83 Bedke, T., Pretsch, L., Karakhanova, S., Enk, A.H. and Mahnke, K. (2010) Endothelial cells augment the suppressive function of CD4^{+}CD25^{+}Foxp3^{+} regulatory T cells: involvement of programmed death-1 and IL-10. *The Journal of Immunology* **184**, 5562–5570 https://doi.org/10.4049/jimmunol.0902458 PMID: 20382886

84 Vignali, D.A.A., Collison, L.W. and Workman, C.J. (2008) How regulatory T cells work. *Nat. Rev. Immunol.* **8**, 523–532 https://doi.org/10.1038/nri2343 PMID: 18566595

85 Francisco, L.M., Salinas, V.H., Brown, K.E., Vanguri, V.K., Freeman, G.J., Kuchroo, V.K. et al. (2009) PD-L1 regulates the development, maintenance, and function of induced regulatory T cells. *J. Exp. Med.* **206**, 3015–3029 https://doi.org/10.1084/jem.20090847 PMID: 20008522

86 Sega, E.I., Leveson-Gower, D.B., Florek, M., Schneidawind, D., Luong, R.H. and Negrin, R.S. (2014) Role of lymphocyte activation gene-3 (lag-3) in conventional and regulatory T cell function in allogeneic transplantation. *PLoS ONE* **9**, e86551 https://doi.org/10.1371/journal.pone.0086551 PMID: 24475140

87 Nikolic, B., Lee, S., Bronson, R.T., Grusby, M.J. and Sykes, M. (2000) Th1 and Th2 mediate acute graft-versus-host disease, each with distinct end-organ targets. *J. Clin. Invest.* **105**, 1289–1298 https://doi.org/10.1172/JCI7894 PMID: 10792004

88 Delens, L., Ehx, G., Somja, J., Vrancken, L., Belle, L., Seidel, L, et al. (2019) *In vitro* Th17-polarized human CD4^{+} T cells exacerbate xenogeneic graft-versus-host disease. *Biol. Blood Marrow Transplant* **25**, 204–215 https://doi.org/10.1016/j.bbmt.2018.10.007 PMID: 30326279

89 Carlson, M.J., West, M.L., Coghill, J.M., Panoskaltsis-Mortari, A., Blazar, B.R. and Serody, J.S. (2009) *In vitro*-differentiated TH17 cells mediate lethal acute graft-versus-host disease with severe cutaneous and pulmonary pathologic manifestations. *Blood* **113**, 1365–1374 https://doi.org/10.1182/blood-2008-06-162420 PMID: 18957685

90 Serody, J.S. and Hill, G.R. (2012) The IL-17 differentiation pathway and its role in transplant outcome. *Biol. Blood Marrow Transplant.* **18**, S56–61 https://doi.org/10.1016/j.bbmt.2011.10.001 PMID: 22226114

91 Roy, J., Platt, J.L. and Weisdorf, D.J. (1993) The immunopathology of upper gastrointestinal acute graft-versus-host disease. Lymphoid cells and endothelial adhesion molecules. *Transplantation* **55**, 572–578 https://doi.org/10.1097/00007890-199303000-00022 PMID: 7681225

92 Tanaka, M., Umihara, J., Shimmoto, K., Cui, S.J., Sata, H., Ishikawa, T. et al. (1989) The pathogenesis of graft-versus-host reaction in the intrahepatic bile duct. An immunohistochemical study. *Acta Pathol. Jpn.* **39**, 648–655 https://doi.org/10.1111/j.1440-1827.1989.tb02412.x PMID: 2686350

93 Kim, S.Y., Lee, H., Han, M.-S., Shim, H., Eom, H.-S., Park, B, et al. (2016) Post-transplantation natural killer cell count: a predictor of acute graft-versus-host disease and survival outcomes after allogeneic hematopoietic stem cell transplantation. *Clin. Lymphoma. Myeloma Leuk* **16**, 527–535 https://doi.org/10.1016/j.clml.2016.06.013 PMID: 27375156

94 Larghero, J., Rocha, V., Porcher, R., Filion, A., Ternaux, B., Lacassagne, M.-N. et al. (2007) Association of bone marrow natural killer cell dose with neutrophil recovery and chronic graft-versus-host disease after HLA identical sibling bone marrow transplants. *Br. J. Haematol.* **138**, 101–109 https://doi.org/10.1111/j.1365-2141.2007.06623.x PMID: 17555453

95 Tanaka, M., Kobayashi, S., Numata, A., Tachibana, T., Takasaki, H., Maruta, A. et al. (2012) The impact of the dose of natural killer cells in the graft on severe acute graft-versus-host disease after unrelated bone marrow transplantation. *Leuk. Res.* **36**, 699–703 https://doi.org/10.1016/j.leukres.2011.11.009 PMID: 22172462

96 McCurdy, S.R., Radojcic, V., Tsai, H.-L., Vulic, A., Thompson, E., Ivcevic, S. et al. (2022) Signatures of GVHD and relapse after posttransplant cyclophosphamide revealed by immune profiling and machine learning. *Blood* **139**, 608–623 https://doi.org/10.1182/blood.2021013054 PMID: 34657151

97 Mu, H., Konopleva, M., Jacamo, R., Carter, B.Z., McQueen, T. and Andreeff, M. (2017) Comparison of induction chemotherapy in NSG and NOD- Rag1 ^{null} IL2rg ^{null} mouse models of FLT3 mutant AML. *Blood* **130**, 2692–2692 https://doi.org/10.1182/blood.V130.Suppl_1.2692.2692

© 2025 The Author(s). This is an open access article published by Portland Press Limited on behalf of the Biochemical Society and distributed under the Creative Commons Attribution License 4.0 (CC BY).

98 Salas, M.Q., Cascos, E., López-García, A., Pérez-López, E., Baile-González, M., López-Corral, L. et al. (2024) Cardiac events occurring after allogeneic hematopoietic cell transplantation with post-transplant cyclophosphamide. Study conducted on behalf of the GETH-TC. *Bone Marrow Transplant.* **59**, 1694–1703 https://doi.org/10.1038/s41409-024-02414-z PMID: 39277653

99 Salerno, N., Di Costanzo, A., Marino, F., Scalise, M., Leo, I., Sabatino, J. et al. (2025) Echocardiographic assessment of cardiac function in mouse models of heart disease. *Int. J. Mol. Sci.* **26**, 5995 https://doi.org/10.3390/ijms26135995 PMID: 40649774

100 Hou, H., Yang, Y., Zhu, M., Xie, M., Zhang, Y. and Chen, R. (2025) Osthole attenuates trastuzumab-induced cardiotoxicity in mice by enhancing autophagy via regulating the p38MAPK/mTOR signaling pathway. *J. Tradit. Complement. Med.* https://doi.org/10.1016/j.jtcme.2025.06.001

101 Augé, C., Gamé, X., Vergnolle, N., Lluel, P. and Chabot, S. (2020) Characterization and validation of a chronic model of cyclophosphamide-induced interstitial cystitis/bladder pain syndrome in rats. *Front. Pharmacol.* **11**, 1305 https://doi.org/10.3389/fphar.2020.01305 PMID: 32982733

102 Ramaiah, S.K. (2007) A toxicologist guide to the diagnostic interpretation of hepatic biochemical parameters. *Food Chem. Toxicol.* **45**, 1551–1557 https://doi.org/10.1016/j.fct.2007.06.007 PMID: 17658209

103 Ezhilarasan, D., Karthikeyan, S., Najimi, M., Vijayalakshmi, P., Bhavani, G. and Jansi Rani, M. (2025) Preclinical liver toxicity models: advantages, limitations and recommendations. *Toxicology* **511** https://doi.org/10.1016/j.tox.2024.154020 PMID: 39637935

104 Al-Naimi, M.S., Rasheed, H.A., Hussien, N.R., Al-Kuraishy, H.M. and Al-Gareeb, A.I. (2019) Nephrotoxicity: role and significance of renal biomarkers in the early detection of acute renal injury. *J. Adv. Pharm. Technol. Res.* **10**, 95–99 https://doi.org/10.4103/japtr.JAPTR_336_18 PMID: 31334089

© 2025 The Author(s). This is an open access article published by Portland Press Limited on behalf of the Biochemical Society and distributed under the Creative Commons Attribution License 4.0 (CC BY).